Copyright © 1986, by the author(s).
All rights reserved.

Permission to make digital or hard copies of all or part of this work for personal or classroom use is granted without fee provided that copies are not made or distributed for profit or commercial advantage and that copies bear this notice and the full citation on the first page. To copy otherwise, to republish, to post on servers or to redistribute to lists, requires prior specific permission.

MODELING CONSIDERATIONS FOR BIPOLAR TRANSISTORS

by

J. David Burnett

Memorandum No. UCB/ERL M86/72

2 September 1986

MODELING CONSIDERATIONS FOR BIPOLAR TRANSISTORS

by

J. David Burnett

Memorandum No. UCB/ERL M86/72

2 September 1986

ELECTRONICS RESEARCH LABORATORY

College of Engineering
University of California, Berkeley
94720

MODELING CONSIDERATIONS FOR BIPOLAR TRANSISTORS

by

J. David Burnett

Memorandum No. UCB/ERL M86/72

2 September 1986

ELECTRONICS RESEARCH LABORATORY

College of Engineering
University of California, Berkeley
94720

ABSTRACT

Tradeoffs between model accuracy and simulation time of bipolar junction transistor models have been investigated. The Gummel-Poon model has been compared to the Turgeon-Mathews model by implementing both models into the circuit simulator BIASC.

The Turgeon-Mathews model contains more accurate approximations for basewidth modulation and high-injection effects in the transistor than the Gummel-Poon model. Included in the Turgeon-Mathews model are specific equations for modeling quasi-saturation effects (high-injection effects in the epitaxial collector). The Turgeon-Mathews model requires more parameters and also contains more equations than the Gummel-Poon model.

The performance of the models has been compared by using each model to generate the dc characteristics of a shallow-base, high-voltage device. The Turgeon-Mathews model provides a better fit to the device characteristics than the Gummel-Poon model while requiring approximately 60% more time for the model evaluation.

This research was partially supported by National Semiconductor.

ACKNOWLEDGEMENTS

The author would like to thank Professor D.O. Pederson for his support and patience during the course of this research.

Discussions with L. Turgeon are greatly appreciated as well as his encouragement.

The support of the fellow workers in the author's research group. Ron. Karti. George. and Theo is especially appreciated as well as the support of other Berkeleyite EE's — Res. Jeff. Carl. Ellen. Reng Song. Dev. Greg. Giorgio. Fabio. and Chuck.

The author thanks Mike. Stuart. and Ted for their friendships. encouragement. and participation in attitude adjustment pursuits. his family for their love and support. and Carmen for giving life some additional meaning and excitement.

The author is grateful to Professor P.E. Allen for interesting him in continuing his education at Berkeley.

The support of Tektronix for supplying data is acknowledged.

Finally. the author thanks Berke Breathed for helping him to start off every day with a laugh and for keeping life in a proper perspective.

TABLE OF CONTENTS

CHAPTER 1: INTRODUCTION 1

CHAPTER 2: THE SPICE GUMMEL-POON MODEL 4

2.1 Introduction 4

2.2 Model Equations 4

2.3 Deficiencies of the Gummel-Poon Model 7

2.3.1 Basewidth Modulation 9

2.3.2 High-Level Injection 10

2.4 Dynamic Performance 13

CHAPTER 3: THE TURGEON-MATHEWS MODEL 14

3.1 Introduction 14

3.2 The Base Region 15

3.2.1 High Injection for a PN Junction 18

3.2.2 Base Majority Carrier Concentration 20

3.3 The Collector Region 23

3.3.1 The Modulated Intrinsic Collector Resistance 24

3.3.2 Recombination Current in the Collector Region 27

3.4 Dynamic Equations 28

3.5 Current Crowding in the Collector 29

3.6 Model Parameters 30

CHAPTER 4: RESULTS 34

4.1 Introduction 34

4.2 Accuracy 34

4.2.1 The Gummel-Poon Model 37

4.2.2 The Turgeon-Mathews Model 37

4.3 Speed of Evaluation 42

4.4 Conclusions 43

4.5 Future Work 43

APPENDIX A: EPITAXIAL COLLECTOR RESISTANCE MODULATION 46

APPENDIX B: RECOMBINATION CURRENT IN THE COLLECTOR REGION 48

APPENDIX C: COLLECTOR REGION STORED CHARGE 50

APPENDIX D: PN JUNCTION EXPRESSION FOR HIGH INJECTION 50

APPENDIX E: BASE TRANSPORT CURRENT 52

APPENDIX F: LISTING OF THE GUMMEL-POON MODEL FUNCTION 57

APPENDIX G: LISTING OF THE TURGEON-MATHEWS MODEL FUNCTION 65

REFERENCES 78

CHAPTER 1

INTRODUCTION

In recent years there has been a resurgence in bipolar integrated circuit technology in both analog and digital design due primarily to reductions in both the horizontal and vertical dimensions of the bipolar transistor. These reductions allow modern bipolar transistors to be operated over increasingly larger ranges of current densities. For large-scale-integration applications. the transistor is operated at very low current densities. while for high-speed functions the transistor is operated at much higher current densities. The structure of the bipolar device also varies depending upon the application for which it will be used. For high-voltage devices a thick. lightly doped epitaxial collector is used. while for high-frequency devices the basewidth is very narrow. Some devices use polysilicon to contact to the emitter. base. and collector to reduce the extrinsic (nonactive) portion of the transistor.

Because of the wide range of operation and application. it is important for bipolar models used in integrated circuit simulation programs to be as robust (with respect to accuracy) as possible. For the bipolar junction transistor model in the circuit simulator Spice [Nag75]. a modified version of the Gummel-Poon model [Gum70b] is used. Despite many advancements in bipolar technology. this version has remained virtually unchanged over the past ten years indicating a good correspondence of the model to the physical device. Of course. there are limitations to the model and this can result in the use of a different set of model parameters for the dc. ac. and transient analyses of a transistor. For a physically derived (analytical) model. such as the GP (Gummel-Poon) model. to improve the accuracy of the model implies that certain effects cannot be neglected or approximated and must be incorporated into the model in some fashion.

This generally results in complicated equations that include new physical effects. The analytic equations become more complex, resulting in increased model evaluation time. This report considers the limitations of the Gummel-Poon model, ways to improve some of these limitations, and the price paid for these improvements.

The model that appears in Chapter 3 was developed by Turgeon and Mathews of Bell Labs [Tur80],[Tur86]. This model is similar to the GP model in that both use a integral charge-control relation. The TM (Turgeon-Mathews) model incorporates an expression for high injection at a pn junction throughout their derivation which is not accounted for by the GP model. This results in a different implementation of the base-charge expression from the GP model and in specific equations for modeling quasi-saturation effects (high-injection effects in the epitaxial collector). To obtain a robust model for narrow basewidth transistors, the base-charge expression must be accurate over a large range of current density and bias: In high-voltage transistors, quasi-saturation effects are prominent and result in reduced collector resistance, current gain (β), and cutoff frequency (f_T) [Mac82], [War85], [Whi69]. Except for lifetime-dependent parameters, the TM model parameters are extractable from the doping profile and geometry of the device resulting in the capability to perform predictive modeling (the effect of changes in process and device technology upon circuit performance without first producing a prototype [Kne85]) and to simulate the performance under worst-case process variations.

To investigate the accuracy and computational efficiency of these two models, both have been implemented into BIASC [Gyu85], a circuit simulator written in the "C" programming language, and have been used to generate the dc characteristics for a shallow-base, high-voltage device. The nature of this device, that of a narrow base and a lightly-doped, thick collector, presents a difficult challenge for accurate modeling.

The remaining chapters of this report are organized as follows: Chapter 2 contains the dc portion of the Gummel-Poon model and addresses several of its limitations; the Turgeon-Mathews model is presented in Chapter 3 with particular attention to the limitations noted in the previous chapter; and the report concludes with Chapter 4 which contains the results.

CHAPTER 2

THE SPICE GUMMEL-POON MODEL

2.1. INTRODUCTION

This chapter reviews the Gummel-Poon model (GP) as implemented in the SPICE circuit simulation program. The first section provides equations for the dc part of the GP model. In Section 2 certain deficiencies in the model are noted by indicating some of the effects of the assumptions made in the model derivation. Considerations regarding the modeling for ac and transient analyses are briefly covered. For further explanation of the GP model derivation along with a description of the Ebers-Moll model. [Get76] is an excellent book to consult.

2.2. MODEL EQUATIONS

The beginning point of the GP model is the transport version of the Ebers-Moll equations describing the bipolar transistor action, as shown in Figure 2.1.

The collector and emitter currents. I_C and I_E. are given by

$$I_C = I_{CC} - I_{BC} \tag{2.1}$$

$$I_E = -I_{CC} - I_{BE} \tag{2.2}$$

where I_{CC} is the transported current and I_{BE} and I_{BC} are recombination currents that comprise the base current I_B.

From this starting point. the GP model adds another recombination current component for both I_{BE} and I_{BC} and incorporates a normalized conductivity modulated base charge. q_b. into the transport current expression [Gum70a]. [Mul77] resulting in the following current components:

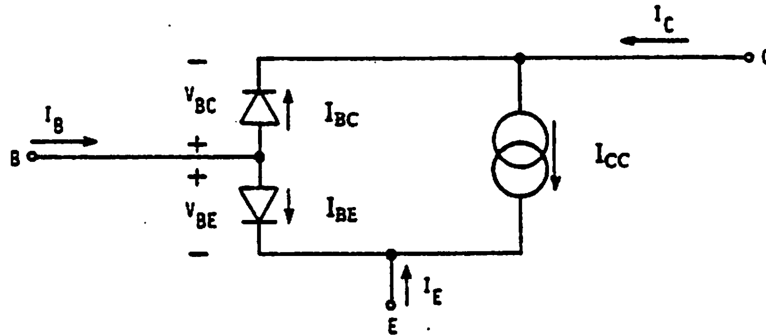

$$I_{CC} = I_S \left[(e^{V_{be}/V_t} - 1) - (e^{V_{bc}/V_t} - 1) \right] \quad (2.3)$$

$$I_{BC} = \frac{I_S}{\beta_R}(e^{V_{bc}/V_t} - 1) \quad (2.4)$$

$$I_{BE} = \frac{I_S}{\beta_F}(e^{V_{be}/V_t} - 1) \quad (2.5)$$

Figure 2.1. Ebers-Moll Equations in Transport Form

$$I_{CC} = \frac{I_S(e^{V_{be}/V_t} - e^{V_{bc}/V_t})}{q_b(V_{be}, V_{bc})} \quad (2.6)$$

$$I_{BE} = \frac{I_S}{\beta_F}(e^{V_{be}/V_t} - 1) + I_{SE}(e^{V_{be}/n_e V_t} - 1) \quad (2.7)$$

$$I_{BC} = \frac{I_S}{\beta_R}(e^{V_{bc}/V_t} - 1) + I_{SC}(e^{V_{bc}/n_c V_t} - 1) \quad (2.8)$$

where $q_b = \frac{Q_b}{Q_{bo}} = 1 + q_{je} + q_{jc} + q_{de} + q_{dc}$. ($q_b$ is explained in more detail in the next section.) The terms q_{je} and q_{jc} represent the junction charge-storage elements for the base-emitter and base-collector junctions, respectively and are given by

$$q_{je} = \frac{V_{be}}{V_B} \tag{2.9}$$

$$q_{jc} = \frac{V_{bc}}{V_A} \tag{2.10}$$

The terms q_{de} and q_{dc} represent the diffusion charge-storage and are given by

$$q_{de} = \frac{I_S}{I_{KF}} \frac{(e^{V_{be}/V_t} - 1)}{q_b} \tag{2.11}$$

$$q_{dc} = \frac{I_S}{I_{KR}} \frac{(e^{V_{bc}/V_t} - 1)}{q_b} \tag{2.12}$$

The expression for q_b can be simplified to a quadratic equation by defining

$$q_1 = 1 + q_{je} + q_{jc} \tag{2.13}$$

$$q_2 = (q_{de} + q_{dc})q_b \tag{2.14}$$

so that

$$q_b = q_1 + \frac{q_2}{q_b} \tag{2.15}$$

and solving for q_b yields

$$q_b = \frac{q_1}{2} + \sqrt{(\frac{q_1}{2})^2 + q_2} \tag{2.16}$$

Then, assuming that $q_1 >> q_2$,

$$q_b \approx \frac{q_1}{2}\left[1 + \sqrt{1 + 4q_2}\right] \tag{2.17}$$

q_1 is further modified by assuming that $V_{be} << V_B$ and $V_{bc} << V_A$ so that

$$q_1 \approx \frac{1}{1 - \frac{V_{be}}{V_B} - \frac{V_{bc}}{V_A}} \tag{2.18}$$

The base resistance is expressed as the sum of a constant external resistance, $R_{b,ext}$, and a modulated internal resistance, $R_{b,int}$. $R_{b,ext}$ represents the resistance from the base contact to the periphery of the base-emitter junction and $R_{b,int}$ corresponds to the resistance under the emitter and is modulated by the base charge as $R_{b,int} = R_{b,int,max}/q_b$. (A more complicated expression for R_b, based upon [Hau64], can be used as explained in the Spice manual.) With the addition of the two ohmic

resistances, R_e, and R_c, the above equations define the dc portion of the GP model.

2.3. DEFICIENCIES OF THE GUMMEL-POON MODEL

It is in the implementation of the base charge that certain limitations can be noted. The modulated base charge expression, q_b, represents the total amount of majority charge in the active base, Q_b, normalized to the majority base charge with zero bias (the equilibrium amount), Q_{bo}.

$$q_b = \frac{Q_b}{Q_{bo}} \tag{2.19}$$

where

$$Q_b = qA\int_{x_e}^{x_c} p(x)dx \tag{2.20}$$

and

$$Q_{bo} = qA\int_{x_{eo}}^{x_{co}} p(x)dx \tag{2.21}$$

with reference to Figure 2.2. (Although the integration above is from the depletion edges inside the base, the original Gummel-Poon paper integrated across the entire transistor and included both space charge regions. [Get76] indicates that this difference is negligible.) Figure 2.2 illustrates the majority charge, holes for this example, in the base of a transistor with both the base-emitter and base-collector junctions forward biased. The total majority charge is represented by $p(x)$ and at zero bias $p(x) = N_A(x)$, the doping concentration in the base. As V_{be} and V_{bc} vary, the depletion widths of each junction change resulting in the modulation of the active basewidth, W_B. The charge representing the change from zero-bias of ionized donor-electron or acceptor-hole pairs is termed the depletion charge, Q_{je} for the base-emitter junction and Q_{jc} for the base-collector junction. Also, as V_{be} and V_{bc} change from zero bias, there is a charge associated with the forward and reverse injection of base-

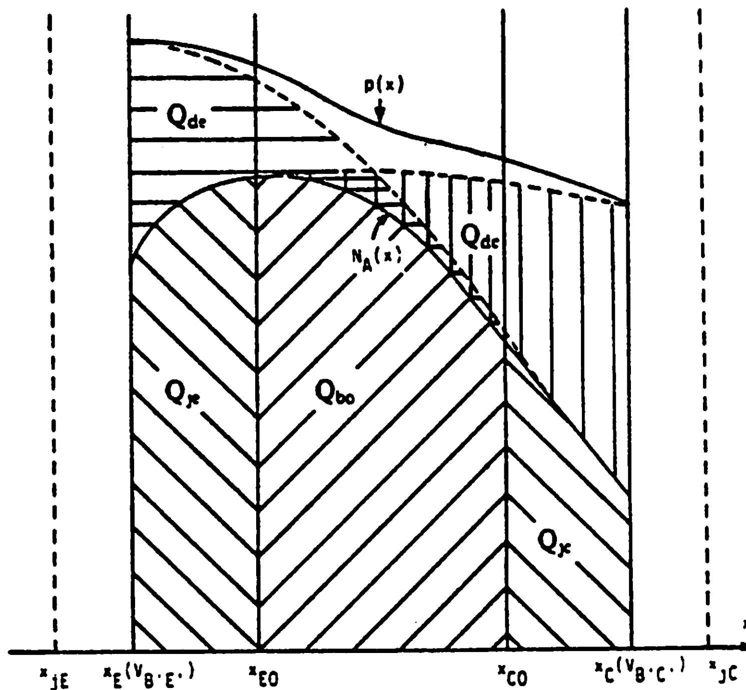

Figure 2.2. The Base Majority Charge

minority carriers. Since charge neutrality is maintained in the base, the excess majority carrier concentration equals the excess minority carrier concentration. This excess charge is called the diffusion charge, with Q_{de} and Q_{dc} corresponding to injection from the base-emitter and from the base-collector junctions, respectively, and represents the change in free electron-hole pairs from zero bias.

The deficiencies of the implementation are: (1) basewidth modulation is not accurately modeled over a large bias range, and (2) high-injection is only modeled to allow β to roll-off as $\frac{1}{I_c}$. Both of these deficiencies are elaborated upon in more detail below.

2.3.1. Basewidth Modulation

As the width of the base modulates with bias, the amount of charge stored in the junction depletion regions changes (Q_{je} and Q_{jc} in Figure 2.2.). This depletion charge is modeled in the q_1 portion of q_b as

$$q_1 = \frac{Q_{bo} + Q_{je} + Q_{jc}}{Q_{bo}} = 1 + q_{je} + q_{jc} \tag{2.22}$$

Since the junction depletion capacitance is related to the junction depletion charge and voltage by $C_j = \frac{dQ}{dV}$, for the base-emitter junction

$$Q_{je} = \int_0^{V_{be}} C_{je}(V)dV \tag{2.23}$$

$$q_{je} = \frac{1}{Q_{bo}} \int_0^{V_{be}} C_{je}(V)dV \tag{2.24}$$

Making the assumption that C_{je} is constant and equal to an average value $C_{je,avg}$, gives

$$q_{je} = \frac{C_{je,avg} V_{be}}{Q_{bo}} = \frac{V_{be}}{V_B} \tag{2.25}$$

where V_B, the inverse Early Voltage, is

$$V_B = \frac{Q_{bo}}{C_{je,avg}} \tag{2.26}$$

Similarly, for the base-collector junction

$$q_{jc} = \frac{C_{jc,avg} V_{bc}}{Q_{bo}} = \frac{V_{bc}}{V_A} \tag{2.27}$$

where V_A, the Early Voltage, is

$$V_A = \frac{Q_{bo}}{C_{jc,avg}} \tag{2.28}$$

The assumption above, that an average value, independent of voltage, can be used for the depletion capacitances C_{je} and C_{jc} is most valid for reverse biases on a junction. However, in the forward bias region, the depletion capacitance can change greatly with very little change in bias, implying that the integration using the average capacitance may not accurately represent the integral of the capacitance. If a transistor is only

operated at one bias or a small range of bias, then V_A and V_B for this bias should provide a good tracking of the depletion charges. However, for transient operation, in which the transistor operates over a wide range of voltages and currents, the error can become significant, especially for shallow-base transistors in which the basewidth is so narrow that the depletion charge can approach the zero-bias base charge Q_{bo}. In less advanced transistors with wider bases, Q_{bo} usually dominates the depletion charges so that the errors in the constant-capacitance approximation do not become significant.

2.3.2. High-Level Injection

At high-injection levels, the injection of minority carriers into a neutral region is significant with respect to the majority carrier concentration. In the GP model for high bias, the high-injection effects of q_2 dominate the Early effect associated with q_1 so that q_b approaches $\sqrt{q_2}$. In this high-level condition, $q_b \propto e^{V_{be}/2V_t}$ and $I_C \propto e^{V_{be}/2V_t}$ causing $\beta = \frac{I_C}{I_B}$ to fall-off as $\frac{1}{I_C}$ which agrees with the Webster-Rittner effect [Web54],[Rit54] for high-injection in the base.

However, as seen in the β vs I_C curves of Figure 2.3, β falls off much more rapidly that $\frac{1}{I_C}$ at high-current levels. This is the result of high-injection occurring first in the collector rather than in the base because the collector-epitaxial region is the most lightly doped part of the transistor. The region of operation in which high-injection in the collector occurs is called quasi-saturation and was first explained by Kirk using a base push-out concept [Kir62]. Quasi-saturation occurs when the internal (metallurgical) base-collector junction is forward biased even though the external base-collector junction is reversed biased (refer to Section 3.3 for further elaboration on the concept of quasi-saturation). As indicated in the I_C vs V_{CE} curves of Figure 2.4, the quasi-saturation region bridges the full-saturation and forward-active regions

of operation and results in a reduced collector current compared to the forward active collector current given the same base current. Further, when high-injection occurs in the collector, the epitaxial region is conductivity modulated resulting in collector resistance modulation, carrier recombination, and stored charge, none of which are modeled in the GP model. Although these effects might seem restrictive, the effects of high-injection in the collector are much less severe when the epitaxial region is not lightly doped and, since β and f_T fall-off rapidly in quasi-saturation, transistors are usually not operated in this mode.

β fall-off due to high-injection in the base is modeled using the base diffusion charge expression, q_2. However, in the derivation of q_2, constant transit times are assumed which further limit the modeling capabilities. The excess diffusion charge is divided into forward and reverse current-controlled components:

$$q_2 = \frac{\tau_f I_f - \tau_r I_r}{Q_{bo}} \tag{2.29}$$

where

$$I_f = \frac{I_S(e^{V_{be}/V_t} - 1)}{q_b} \tag{2.30}$$

and

$$I_r = \frac{I_S(e^{V_{bc}/V_t} - 1)}{q_b} \tag{2.31}$$

so that $I_f - I_r = I_{CC}$. Here τ_f and τ_r are forward and reverse transit times and are assumed to be constant. By defining

$$I_{KF} = \frac{Q_{bo}}{\tau_f} \tag{2.32}$$

and

$$I_{KR} = \frac{Q_{bo}}{\tau_r} \tag{2.33}$$

q_2 obtains its final form shown in Equation (2.14).

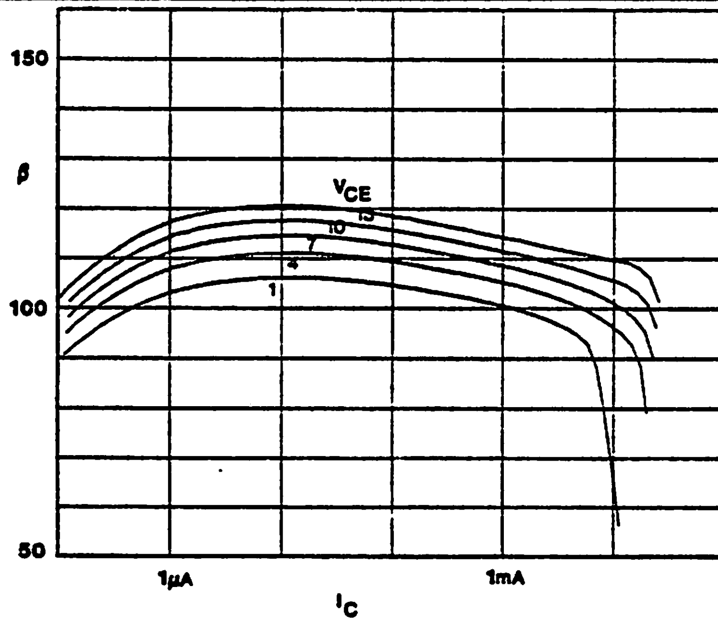

Figure 2.3. β vs I_C Curves at Various V_{CE}

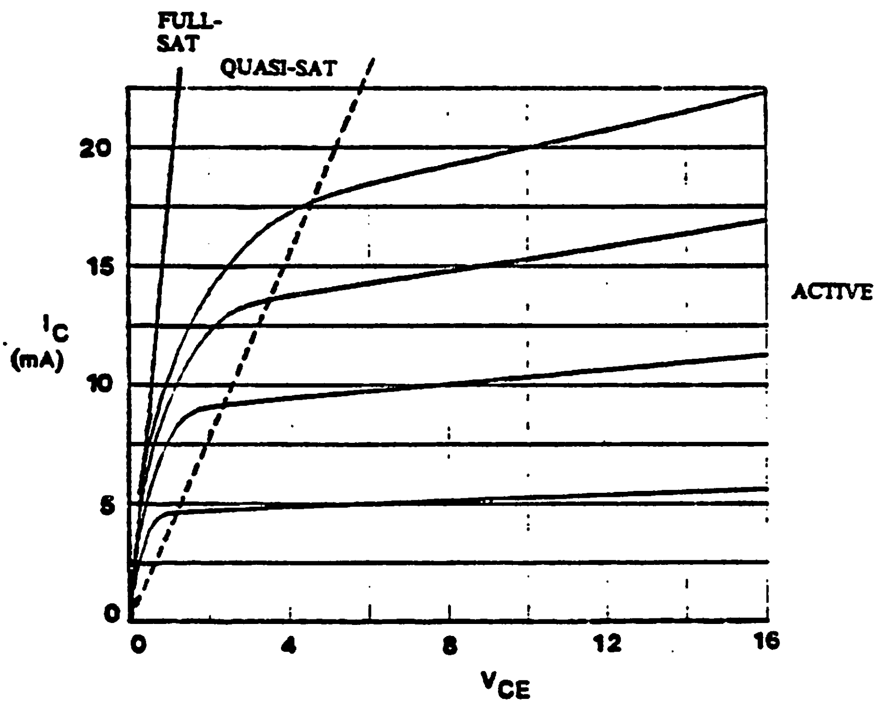

Figure 2.4. I_C vs V_{CE} Curves at Various I_B

As pointed out in [Get76], τ_f includes not only the base transit time, τ_b, but also the emitter-base space-charge layer transit time. Likewise, τ_r includes the collector-base space-charge layer transit time as well as the reverse base transit time. The base transit time [Mul77] and the space-charge layer transit time modulate with both bias and basewidth. Hence, the assumption of constant transit times limits the ability of using one I_{KF} and one I_{KR} for modeling over a large range of bias.

2.4. DYNAMIC PERFORMANCE

Since the results presented in Chapter 4 compare the dc characteristics, the dynamic modeling limitations are only described briefly. One interesting comment regarding the dynamic capabilities of the GP model is contained in the original paper by Gummel and Poon stating that their paper considers mainly the dc and low-frequency aspects of the model and that the model for use in ac or transient analysis would be presented elsewhere.

Because the base-charge expression assumes bias-independent transit times, the dynamic modeling capabilities are limited. One result of this is that both maximum β and maximum f_T are modeled by one parameter, I_{KF} [Sch77]. To aid the modeling of f_T an empirical expression used in curve-fitting the f_T of a high-frequency device was added in 1975 to the diffusion capacitance expression producing improved results. Another deficiency is the modeling of the forward-biased junction capacitance by using a straight line approximation [Sch77]. This problem can be reduced by using one extra model parameter as shown in [Poo69]. Finally, due to the lack of quasi-saturation modeling, the stored charge at high-injection levels in the collector that results in a severe f_T drop is not modeled.

CHAPTER 3

THE TURGEON-MATHEWS MODEL

3.1. INTRODUCTION

The Turgeon-Mathews model (TM) contains charge-controlling expressions as does the Gummel-Poon model. While the GP model considers only charge in the base region (the original GP derivation included a base-widening factor that extended the base region into the collector), the TM model implements both base and collector charge expressions. The TM base region derivation is very similar to that of the GP model as both models contain a base transport current that is developed in terms of a base charge which is partitioned into depletion and diffusion charges and as both models include similar recombination current terms for the base region. In the base region, the TM model differs from the GP model in the implementation of the depletion and diffusion charges in the base charge expression and by incorporating explicitly high-injection terms into each of the base current expressions. In the collector region, Turgeon and Mathews model high injection by modulating the collector epitaxial resistance, including a recombination current for the excess minority carriers, and calculating the corresponding stored charge. The resulting model equations are coupled very closely to the device physics and, hence, the model parameters, except for the lifetime dependent parameters, are extractable from the doping profile and geometry of the device.

Contained in Appendices A through E are the derivations of the significant concepts of the TM model from [Tur86]. This chapter presents the complete TM model and elaborates on these derivations. The figures and table in this chapter are from

[Tur86].

Figure 3.1a illustrates the cross-sectional view of a typical vertical bipolar transistor. Superimposed on this figure is the symbolic transistor model with the ideal part contained inside the dotted lines. The symbolic model is shown again in Figure 3.1b with the internal junction voltages, V_{bei} and V_{bci}, defined across the transistor junctions and the external voltages, V_{bex}, V_{bcx}, and V_{cex} defined across the terminals. R_c, the epitaxial region collector resistance, in Figure 3.1a is the same resistance as R_{ci} in Figure 3.1b. R_{cx} is the sum of the buried layer resistance, R_{bL}, and the deep collector resistance, R_{dc}.

3.2. THE BASE REGION

The currents associated with the base, collector, and emitter of the device are illustrated in Figure 3.2. The derivation and implementation of the base transport current, I_{CC}, are derived in Appendix E. The base transport current expression, Equation (E.2),

$$I_{CC} = \frac{qA_e D_n (n_e p_e - n_c p_c)}{\int_{x_c}^{x_e} p(x) dx} \tag{3.1}$$

as Turgeon and Mathews indicate, is similar to the standard base-transport equation except for the location of the boundaries x_e and x_c. Figure 3.3 shows a plot of the excess hole carrier density as a function of distance (x) in the vertical direction (for a vertical npn transistor). x_e and x_c correspond to the boundary edges on the base side of the base-emitter and base-collector depletion layers, respectively. For the GP model in [Get76], however, the base charge is integrated from the emitter to collector sides of these depletion regions. But, as Getreu indicates, this difference in the location of boundaries has a negligible effect on the integral of the majority charge. Thus, Equation (3.1) is essentially the same base transport expression used in the GP model.

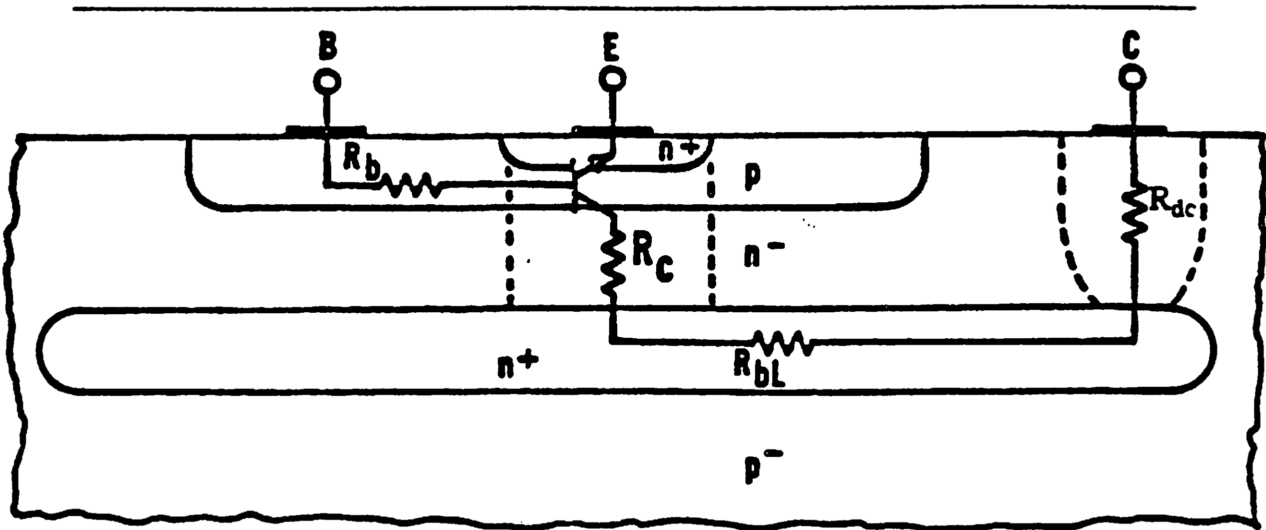

(a)

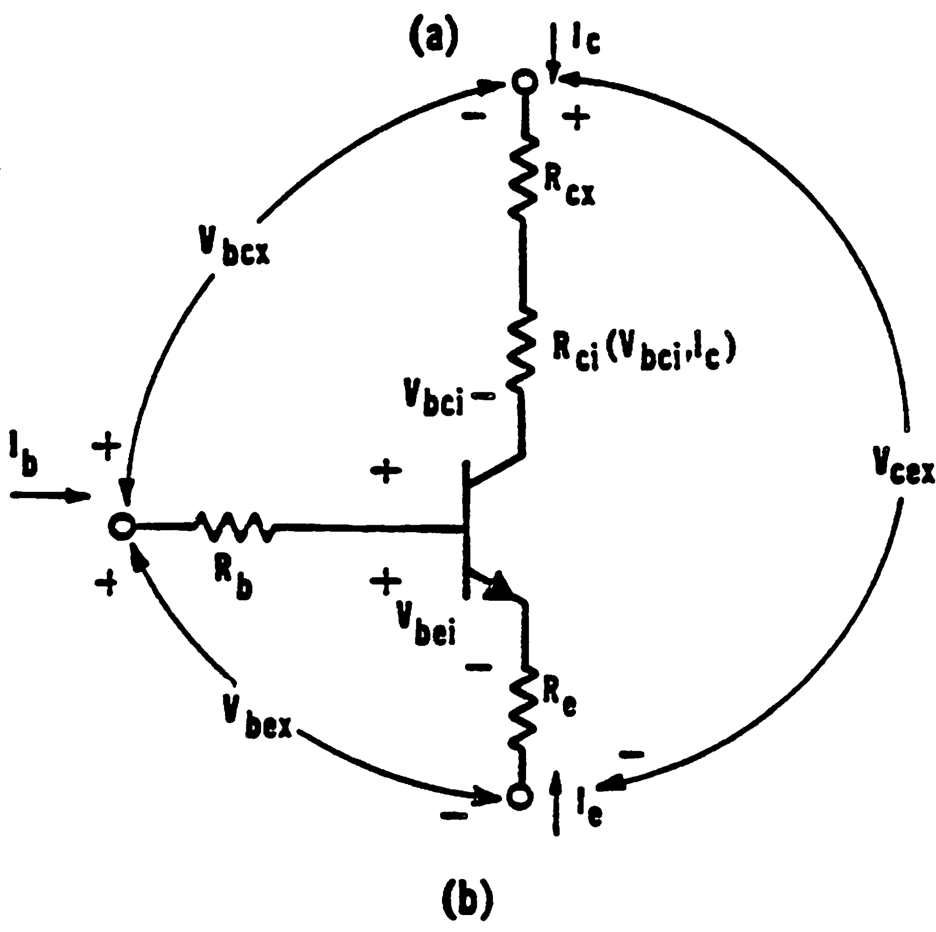

(b)

Figure 3.1. a) Cross-Sectional View of a Vertical Bipolar Transistor
b) Electrical Model of the Bipolar Transistor

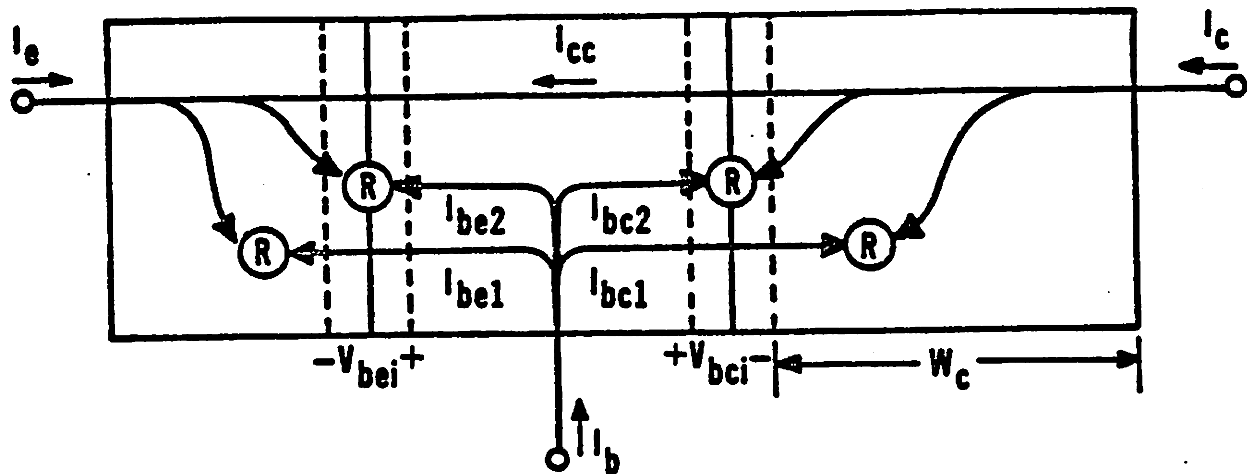

Figure 3.2. Illustration of the Internal Current Paths and Voltages of the Transistor Model.

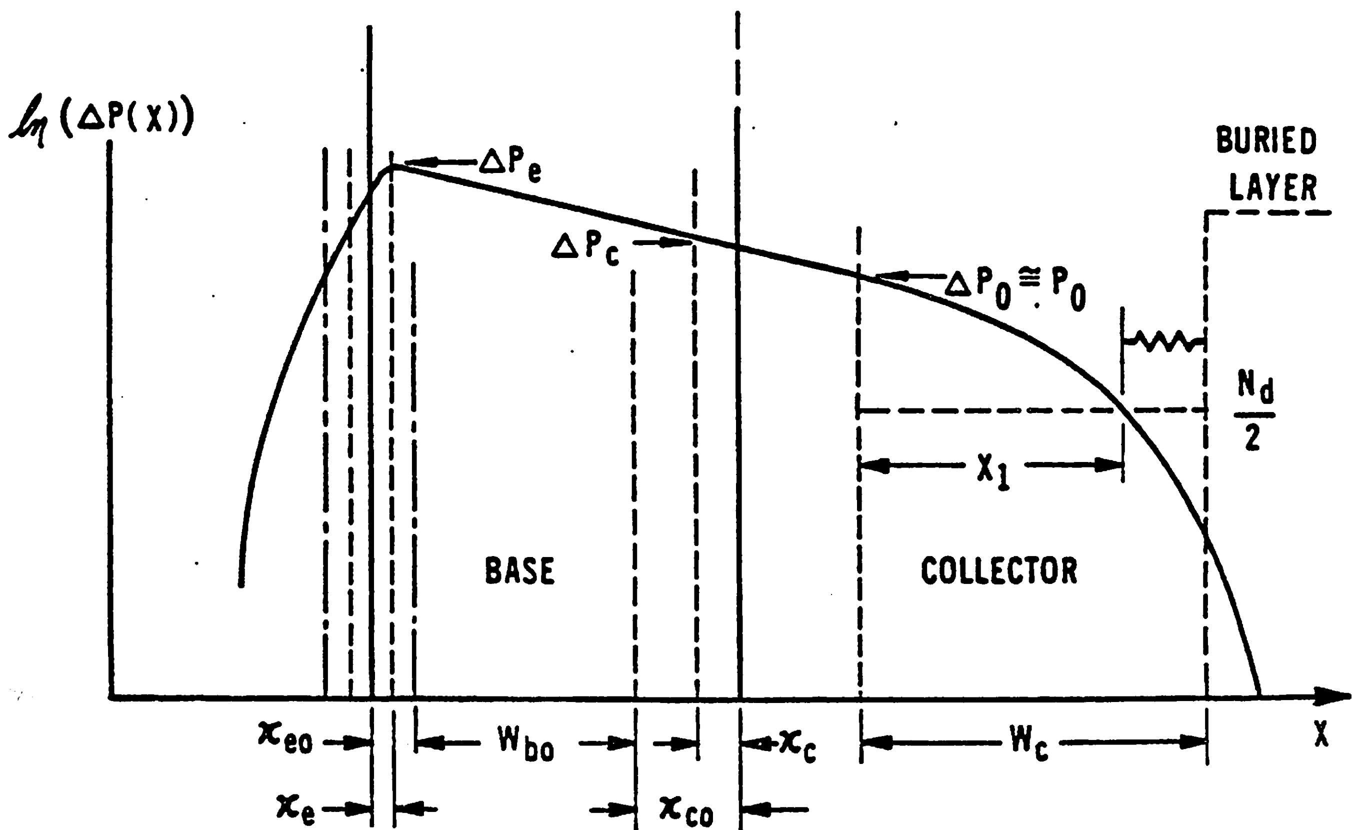

Figure 3.3. Logarithmic Plot of the Excess Hole Carrier Density in the Base and Epitaxial Collector Regions.

Equation (2.6). The implementation of this expression by Turgeon and Mathews, derived in Appendix E, is substantially different from that of Gummel and Poon and incorporates explicitly high injection and basewidth modulation effects.

3.2.1. High Injection for a PN Junction

For the case of low-level injection, the majority carrier concentration does not change substantially from its neutral (doping) concentration. This results in the fami-

liar np product expression

$$np = n_i^2 e^{V_j/V_t} \tag{3.2}$$

Turgeon and Mathews modify the classical np product expression by allowing the majority carrier concentration to modulate and by approximating the junction as being symmetrical. This approximation greatly simplifies the resulting expressions and provides a way of modeling high injection at the junction level. The symmetry approximation is valid for linearly graded junctions and improves under forward bias for asymmetrical junctions.

Resulting from this junction derivation is a high-injection correction factor, $g(V_j)$ in Equation (D.5), that is incorporated into the junction current and junction excess minority carrier expressions (Equations (D.4) and (D.3)). Carrying out this derivation to obtain the np product at the depletion edge results in another high-injection term, $h(V_j)$, defined in Equation (E.4). The final np product expression is

$$np = n_i^2 e^{V_j/V_t} g(V_j) h(V_j) \tag{3.3}$$

Both $g(V_j)$ and $h(V_j)$ are equal to 1 in low-level conditions and become significantly greater than 1 with high levels of injection.

Implementing this expression into the base transport current equation yields

$$I_{CC} = I_S \frac{e^{V_{bei}/V_t} g_e h_e - e^{V_{bci}/V_t} g_c h_c}{q_b(V_{bei}, V_{bci})} \tag{3.4}$$

where the subscripts e and c correspond to the base-emitter and base-collector junctions respectively. Note that if $g_e h_e$ and $g_c h_c$ equal 1 (as they do in low-level injection), then Equation (3.4) is identical to the base transport current expression used in the GP model, Equation (2.6). However, as derived in Appendix E, the implementation of the base majority charge, q_b, is substantially different.

3.2.2. Base Majority Carrier Concentration

As in the GP model, the base charge is partitioned into depletion and diffusion parts along with the built-in charge.

$$Q_b = Q_{bo} + Q_{jc} + Q_{je} + Q_{dc} + Q_{de} \tag{3.5}$$

where Q_{bo} is the built-in charge, Q_{jc} and Q_{je} are the base-collector and base-emitter depletion charges, and Q_{dc} and Q_{de} represent the diffusion charge in the base. q_b is the base charge, Q_b, normalized to Q_{bo}

$$q_b = \frac{Q_b}{Q_{bo}} = 1 + \frac{Q_{jc} + Q_{je} + Q_{dc} + Q_{de}}{Q_{bo}} \tag{3.6}$$

The depletion charges are obtained by integrating the depletion capacitance expression

$$C_j = \frac{C_{jo}}{(1 - \frac{V_j}{\phi_j})^{m_j}} \tag{3.7}$$

to give

$$Q_{je} = \frac{\phi_e C_{jeo}}{(1 - m_e)} \left[1 - (1 - \frac{V_{bei}}{\phi_e})^{1 - m_e} \right] \tag{3.8}$$

$$Q_{jc} = \frac{\phi_c C_{jco}}{(1 - m_c)} \left[1 - (1 - \frac{V_{bci}}{\phi_c})^{1 - m_c} \right] \tag{3.9}$$

The depletion charges are normalized to Q_{bo} to give

$$q_{je} = \frac{Q_{je}}{Q_{bo}} = \frac{\phi_e}{(1 - m_e) V_{BO}} \left[1 - (1 - \frac{V_{bei}}{\phi_e})^{1 - m_e} \right] \tag{3.10}$$

$$q_{jc} = \frac{Q_{jc}}{Q_{bo}} = \frac{\phi_c}{(1 - m_c) V_{AO}} \left[1 - (1 - \frac{V_{bci}}{\phi_c})^{1 - m_c} \right] \tag{3.11}$$

where $V_{AO} = Q_{bo}/C_{jco}$ and $V_{BO} = Q_{bo}/C_{jeo}$ are the forward and reverse Early voltage parameters. As pointed out in Appendix D, because the junction model does not allow the internal junction voltage to exceed the built-in potential, the discontinuities in Equations (3.10) and (3.11) are avoided.

The diffusion charge is evaluated by using a trapezoid from x_e to x_c to approximate the integral of the excess free electron-hole pairs in the base and by assuming that $\Delta n \approx \Delta p$ (charge neutrality in the base). Since the derivation of the base transport current assumes no recombination in the base, the representation of the diffusion charge by a trapezoid is consistent. This concept is expressed in Equation (E.7) and repeated here

$$Q_d = Q_{de} + Q_{dc} = qA_e\left(\frac{\Delta n_e + \Delta n_c}{2}\right)(W_{bo} + \Delta x_{jc} + \Delta x_{je}) \qquad (3.12)$$

where Δx_{jc} and Δx_{jc} are the change in the depletion width of the junctions from zero bias. W_{bo} is the width of the base between the depletion edges at zero bias, and Δn_e and Δn_c are the injected excess electron concentrations at the emitter and collector junction depletion edges inside the base region. At zero bias, Δx_{jc}, Δx_{jc}, Δn_e, and Δn_c are zero.

Equation (D.3) is used in a slightly modified form for representing Δn_e and Δn_c in Equation (3.12). Because of the direct proportionality of Δn_e and Δn_c in Equation (3.12), it is important to express the dependence of $n_{po} = n_i^2/p_{po}(x)$ on the location of the depletion width which moves with bias. The dependence of p_{po} on the spatial location x is emphasized by the notation $p_{po}(x)$ and is implemented by representing the doping of the base side of a junction using a junction gradient expression

$$p_{po}(x) = a_j x_j = a_j x_{jo}\left(1 - \frac{V_j}{\phi_j}\right)^{m_j} = p_{po}(0)\left(1 - \frac{V_j}{\phi_j}\right)^{m_j} \qquad (3.13)$$

where a_j represents the doping gradient and $p_{po}(0)$ is the doping at the depletion edge at zero bias. Δn_e is expressed as

$$\Delta n_e = \frac{n_i^2}{p_{eo}(x)}(e^{V_{bei}/V_t} - 1)g_e = \frac{n_i^2}{p_{eo}\left(1 - \frac{V_{bei}}{\phi_e}\right)^{m_e}}(e^{V_{bei}/V_t} - 1)g_e \qquad (3.14)$$

where p_{eo} corresponds to the doping at the base depletion edge of the base-emitter junction, $p_{eo}(0)$. Using Equation (3.14) for Δn_e in Equation (3.12) yields

$$Q_{de} = \frac{qA_e \Delta n_e}{2}(W_{bo} + \Delta x_{je} + \Delta x_{jc})$$

$$= \frac{qA_e n_i^2(e^{V_{bei}/V_t} - 1)g_e}{2p_{eo}(1 - \frac{V_{bei}}{\phi_e})^{m_e} W_{bo}} \left[1 + \frac{\Delta x_{jc} + \Delta x_{je}}{W_{bo}} \right] \quad (3.15)$$

The normalized diffusion charge. Q_{de}/Q_{bo}. is

$$\frac{Q_{de}}{Q_{bo}} = \frac{qA_e n_i^2(e^{V_{bei}/V_t} - 1)g_e f_e}{2Q_{bo} p_{eo}}$$

$$= \frac{I_S}{I_{KF}}(e^{V_{bei}/V_t} - 1)g_e f_e \quad (3.16)$$

where $I_{KF} = 2qA_e D_n p_{eo}/W_{bo}$ is the forward knee current. f_e contains the effects of basewidth modulation on the diffusion charge and is expressed as

$$f_e = \frac{1 + \frac{\Delta x_{je} + \Delta x_{jc}}{W_{bo}}}{(1 - \frac{V_{bei}}{\phi_e})^{m_e}} \quad (3.17)$$

Δx_{jc} and Δx_{je} represent the change in the depletion widths that extend into the base and are assumed to equal one-half of the total change in the depletion width.

$$\Delta x_{je} = \frac{1}{2}(x_{je} - x_{jeo}) = \frac{x_{jeo}}{2}\left[1 - (1 - \frac{V_{bei}}{\phi_e})^{m_e} \right] \quad (3.18)$$

Inserting this expression for Δx_{je} and a similar one for Δx_{jc} into Equation (3.17) yields

$$f_e = \frac{1 + \frac{V_{BO}\left[1 - (1 - \frac{V_{bei}}{\phi_e})^{m_e} \right] + V_{AO}\left[1 - (1 - \frac{V_{bci}}{\phi_c})^{m_c} \right]}{2V_p}}{(1 - \frac{V_{bei}}{\phi_e})^{m_e}} \quad (3.19)$$

where $V_{AO} = Q_{bo} x_{jco}/\epsilon A_e$ and $V_{BO} = Q_{bo} x_{jeo}/\epsilon A_e$ are the forward and reverse Early voltage parameters. V_p can be calculated using the punch-through condition that occurs when $Q_{je} + Q_{jc} + Q_{bo} = 0$ and $f_e = f_c = 0$. If the change in the emitter junction depletion width is neglected. V_p is solved from the punch-through condition to be

$$2V_p = V_{AO}\left[-1-\frac{V_{BO}}{V_{AO}}+\left[1+(1-m_c)\frac{V_{AO}}{\phi_c}+\frac{\phi_e}{\phi_c}\frac{V_{AO}}{V_{BO}}\frac{(1-m_c)}{(1-m_e)}\right]^{\frac{m_c}{1-m_c}}\right] \quad (3.20)$$

Similarly, the normalized diffusion charge associated with Δn_c is

$$\frac{Q_{dc}}{Q_{bo}} = \frac{I_S}{I_{KR}}(e^{V_{bci}/V_t}-1)g_c f_c \quad (3.21)$$

where $I_{KR} = 2qA_e D_n p_{co}/W_{bo}$ is the reverse knee current. f_c is identical to f_e except for the replacement of the denominator of Equation (E.9) by $(1-\frac{V_{bci}}{\phi_c})^{m_c}$. Note that while the g and h functions each depend on only one junction bias, the f functions depend on both V_{bei} and V_{bci}: $g_e = g(V_{bei})$, $g_c = g(V_{bci})$, $h_e = h(V_{bei})$, $h_c = h(V_{bci})$, $f_e = f(V_{bei}, V_{bci})$, $f_c = f(V_{bci}, V_{bei})$.

The recombination currents illustrated in Figure 3.2, I_{be1}, I_{be2}, I_{bc1}, I_{bc2}, are implemented as

$$I_{be} = I_1 e^{V_{be}/V_t} g_e + I_2 e^{V_{be}/n_e V_t} g_e \quad (3.22)$$

$$I_{bc} = I_3 e^{V_{bc}/V_t} g_c + I_4 e^{V_{bc}/n_c V_t} g_c + I_{bcc} \quad (3.23)$$

where I_1, I_2, I_3, I_4, η_e, and η_c are lifetime dependent input parameters. (In Figure 3.2, a "R" with a circle indicates recombination.) The term I_{bcc} in Equation (3.23) is the collector epitaxial region recombination current and is expressed in Section 3.3.2. Without I_{bcc} the remaining terms of Equations (3.22) and (3.23) are the same as those in the GP model except that the TM equations have a high-injection correction factor, g_e or g_c, appended to them.

3.3. THE COLLECTOR REGION

The TM model equations that apply specifically to the collector region result in the modeling of the quasi-saturation region of operation. As mentioned in Section 2.3.2., quasi-saturation occurs when the internal (intrinsic) base-collector junction becomes forward biased even though the external (extrinsic) base-collector junction is

reverse biased. To gain some insight into this concept, consider a reverse bias voltage applied across the base-collector contacts in Figure 3.1b. At low current levels the voltage drop across the base and collector resistances is very small and the internal base-collector junction potential is approximately equal to the external applied voltage. As the current level rises, the base and collector resistive voltage drops increase resulting in the decrease of the internal base-collector junction reverse bias. Eventually, when the current level rises enough, the voltage drop across the base and collector resistances is sufficiently large to forward bias the internal base-collector junction and the transistor enters the quasi-saturation region of operation. When the collector epitaxial layer becomes fully modulated, the transistor operates in the full-saturation region and the total collector resistance reduces to the external collector resistance, R_{cx}.

One characteristic of quasi-saturation is a decrease in current gain at large current densities. Turgeon and Mathews attribute this reduction to the forward biasing of the internal base-collector junction which produces a recombination current in the collector epitaxial region and conductivity modulates the epitaxial layer resulting in the modulation of the collector resistance. When the collector epitaxial layer becomes fully modulated, the transistor operates in the full-saturation region. The equations for the recombination current and collector resistance are derived in Appendices A and B and the equation for the stored charge in the epitaxial region is derived in Appendix C.

3.3.1. The Modulated Intrinsic Collector Resistance, R_{ci}

One of the distinctive features of the TM model is the voltage and current dependent collector resistance, $R_{ci}(V_{bci}, I_{cc})$, as indicated in Figure 3.1. This is a dominant feature of quasi-saturation, especially in high sustaining voltage transistors (thick and lightly doped epitaxial layers) where the intrinsic collector resistance can vary by ord-

ers of magnitude during operation [Tur86]. Under low-level conditions in the collector, the ohmic region extends vertically from the collector edge of the base-collector depletion region to the N^-N^+ boundary. This ohmic region is shown in Figure 3.2 to have a length W_c that electrons drift across. When the internal base-collector junction becomes forward biased ($V_{bci} > 0$), the onset of quasi-saturation occurs as the minority carrier concentration (holes for an npn) at the collector edge of the junction exceeds its equilibrium amount. When the injected minority carrier concentration approaches the epitaxial doping level (the low-level majority carrier concentration), the majority carrier concentration increases beyond its equilibrium amount due to charge neutrality resulting in the conductivity modulation of the epitaxial region. A typical operating point in quasi-saturation is illustrated in Figure 3.3 by plotting the excess hole carrier density in the base and epitaxial collector regions. The excess minority carrier concentration is indicated by Δp_0. This figure further reveals how Turgeon and Mathews define the difference between the conductivity modulated and ohmic portions of the epitaxial collector. The x_1 region corresponds to the conductivity modulated portion and the remaining region, $W_c - x_1$, is the ohmic portion. Because Turgeon and Mathews define conductivity modulation to occur when the excess majority carrier density exceeds half of the epitaxial layer doping, x_1 occurs at the point where $\Delta p = N_d/2$.

As derived in Appendix A, to obtain an effective resistance across the epitaxial region, Turgeon and Mathews divide an expression for the voltage across this region by the collector current density. This results in Equation (A.5) and contains both an ohmic and conductivity modulated portion. Further manipulation of this equation yields R_{ci} as a function of normalized distance x_o/W_c.

$$R_{ci} = \begin{cases} R_M & \text{for } \frac{x_o}{W_c} \leq 0 \\ R_M(1 - \frac{x_o}{W_c}) & \text{for } 0 < \frac{x_o}{W_c} < 1 \\ 0 & \text{for } \frac{x_o}{W_c} > 1 \end{cases} \quad (3.24)$$

R_M is the maximum epitaxial collector resistance (corresponds to zero-bias or low-level conditions). x_o / W_c, Equation (A.12), is a function of I_c and V_{bci} and becomes significant when conductivity modulation occurs. The assumption that the onset of conductivity modulation occurs at half the doping concentration leads to the piecewise linear equation for R_{ci} as illustrated by the dashed curve in Figure 3.4.

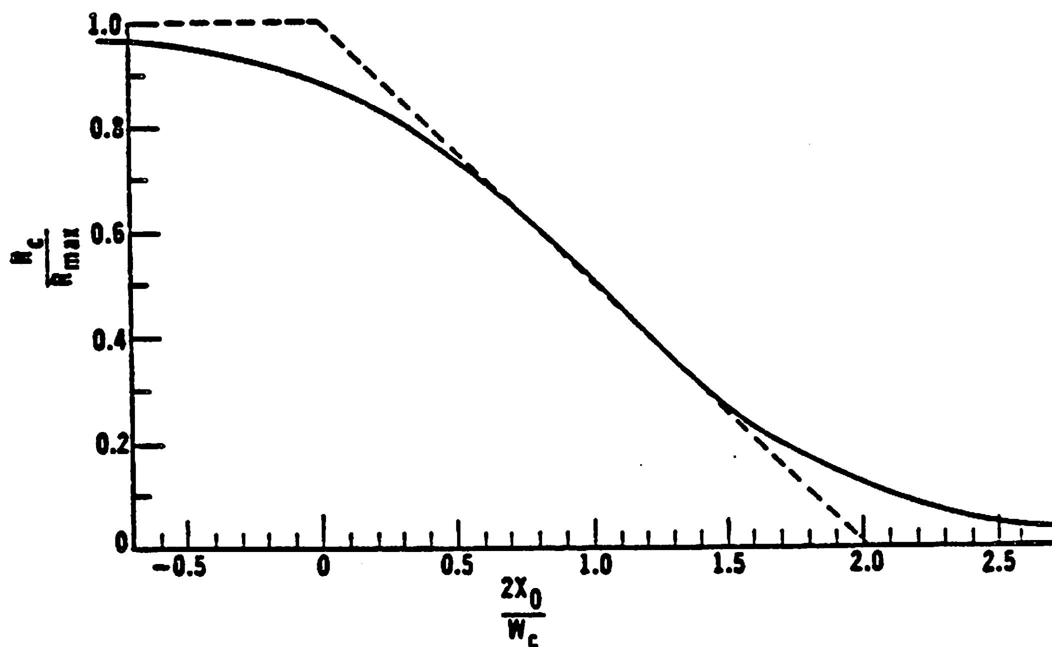

Figure 3.4. Normalized Collector Resistance as a Function of Normalized Distance

For implementation into a circuit simulator, the model equations must be continuous in the first derivative for numerical convergence purposes, so the equation for R_{ci} must be modified. To obtain a smooth version of R_{ci}, Turgeon and Mathews use the following function

$$R_{ci} = \frac{R_M}{1 + \exp[-2(1-2\frac{x_o}{W_c})]} \quad (3.25)$$

This function for R_{ci}, shown as the solid curve in Figure 3.2, fits the piecewise linear model and its derivative exactly at the center of the epitaxial layer ($x_o = W_c/2$) and varies to a maximum deviation of twelve percent at the edges. Not only are numerical convergence problems alleviated by the use of the smooth function, but also the physical representation of the model is improved since the onset of conductivity modulation does not occur abruptly when the carrier concentration equals one half of the doping as assumed in the derivation.

A refinement to Equation (A.12) must be made before implementing it into a circuit simulator. Because I_{CC} is in the denominator of Equation (A.12), I_{CC} cannot be allowed to have a zero value. Turgeon and Mathews avoid this singularity by forcing a lower bound on I_{CC}. This lower bound is introduced by the parameter I_{ccm} that holds I_{CC} independent of bias for $I_{CC} < I_{ccm}$. Turgeon and Mathews use a fifth-order polynomial to smooth out the transition of I_{CC} at I_{ccm}. This mathematical fit is provided in the BIASC program in Appendix G. Because the fit is approximate, I_{ccm} should be chosen to be less than the normal operating current to not introduce errors into the solution.

3.3.2. Recombination Current in the Collector Region

In the quasi-saturation region of operation, some of the base current is due to recombination in the collector epitaxial region. Because this recombination current can

become a significant part of the total base current. Turgeon and Mathews account for it explicitly in their model as a current between the base and collector, I_{bcc}.

The derivation of the recombination current is contained in Appendix B. The resulting expression for I_{bcc}, Equation (B.5) is implemented in a modified form by expressing two new parameters in terms of the parameters I_D^2 and τ_r. By defining $I_5 = I_D^2/I_s\tau_r$ and $I_6 = I_5(3-2/\tau_r)$ Equation (B.5) yields

$$I_{bcc} = \frac{I_S}{I_{CC}}\left[(I_5 - \frac{I_6}{\tau_r})\ln(\tau_r \frac{p_o}{N_{dc}} + 1) + I_6\frac{p_o}{N_{dc}} + I_5(\frac{p_o}{N_{dc}})^2\right] \tag{3.26}$$

where $\tau_r = 2/(3 - I_6/I_5)$. Note that the recombination current expression is proportional to terms involving the minority carrier concentration at the base-collector depletion edge and inversely proportional to the transport current, I_{cc}. In the quasi-saturation region, all of the p_o/N_{dc} terms can potentially dominant the expression and thus they should not be neglected for accurate modeling.

3.4. DYNAMIC EQUATIONS

Although the results presented in Chapter 4 consider only dc characteristics, the stored-charge expressions, which control the dynamic behavior of the transistor model, are included here for completeness.

The junction depletion charges are expressed by multiplying the normalized depletion charges by Q_{bo} which gives

$$Q_{je} = \frac{\phi_e C_{jeo}}{(1-m_e)}\left[1-(1-\frac{V_{bei}}{\phi_e})^{1-m_e}\right] \tag{3.27}$$

$$Q_{jc} = \frac{\phi_c C_{jco}}{(1-m_c)}\left[1-(1-\frac{V_{bci}}{\phi_c})^{1-m_c}\right] \tag{3.28}$$

where C_{jeo} and C_{jco} correspond to the zero-bias capacitance of the base-emitter and base-collector junctions.

Similarly, multiplying the normalized base diffusion charge by Q_{bo} results in

$$Q_{de} = I_S \tau_{fo} e^{V_{be}/V_t} g_e f_e \tag{3.29}$$

$$Q_{dc} = I_S \tau_{ro} e^{V_{bc}/V_t} g_c f_c \tag{3.30}$$

where the transit time parameters $\tau_{fo} = Q_{bo}/I_{KF}$ and $\tau_{ro} = Q_{bo}/I_{KR}$.

Associated with the injection of minority carriers into the epitaxial collector region is a stored charge, Q_c. Turgeon and Mathews obtain this stored charge by integrating the excess minority carrier density in the collector. The stored charge is implemented in an equivalent version of Equation (C.2) as

$$Q_c = \frac{I_S Q_{co}}{I_{CC}} \left[\frac{p_o}{N_{dc}} + \left(\frac{p_o}{N_{dc}}\right)^2 \right] \tag{3.31}$$

where the parameter Q_{co} is defined as $Q_{co} = \tau_{co} I_D^2 / I_S$.

Two important differences in the dynamic equations between the TM and GP models can be noted. Because the junction potential cannot exceed the built-in potential, the need of approximating the forward bias of the depletion capacitance in the GP model is alleviated. Also, as derived at the end of Appendix E, the base transit times are bias dependent with τ_f and τ_r being a function of both V_{bei} and V_{bci}.

3.5. CURRENT CROWDING IN THE COLLECTOR

Current crowding toward the perimeter of the emitter increases with bias with one of its results being the modulation of the base resistance [Mul77]. Further, since the transistor action is vertical, there will also be current crowding effects in the collector. Turgeon and Mathews use an empirical relationship to change the effective area of the collector region as follows:

$$A_e' = \frac{A_e(1 - npc)}{1 + \left(\frac{I_{CC}}{I_{cco}}\right)^{\eta}} + A_e npc \tag{3.32}$$

where I_{cco}, η, and npc are parameters obtained through curve fitting. With $I_{CC} << I_{cco}$,

$A_e' = A_e$, and as I_{CC} becomes larger, the effective area reduces. npc sets a lower bound on how small the effective area can become. Equation (3.29) simulates current crowding by affecting the area dependencies of R_{ci}, I_{bcc}, and Q_{co}.

3.6. MODEL PARAMETERS

Table 3.1 lists the model parameters, with the names of the parameters in the left column, the symbols in the center column, and the expressions that relate the parameters to the doping profile and transistor geometry in the right column. The twenty-nine parameters in this table, along with the curve-fit parameters I_{ccm} (for the I_{CC} term in the R_{ci} expression), and I_{cco}, η_p and npc (for the collector current crowding) are all of the parameters used in the TM model described here. (Additional parameters required to model the distributed base resistance, the distributed base-collector junction capacitance, the collector-substrate junction effects, and temperature effects can be added.) All the parameters that do not depend on carrier lifetime or are not curve-fit parameters can be extracted by the doping profile and transistor geometry.

The parameters I_1, I_2, and η_e account for recombination base current in the emitter, emitter-base space-charge layer, and base regions. These parameters are obtained by fitting to the standard I_B versus V_{be} or β versus log (I_C) characteristics. The parameters I_3, I_4, η_c, I_5, and I_6 represent recombination in the base, base-collector space-charge layer, and collector epitaxial regions. These parameters are obtained by curve-fitting to the quasi-saturation region.

ϕ_e and ϕ_c, the junction built-in potentials, m_e and m_c, the grading coefficients, and C_{jeo} and C_{jco}, the zero-bias junction capacitances, correspond to the use of the depletion and symmetry approximations of a pn junction. The notation associated with the symmetry approximation is that the net doping for a pn junction is $N = ax^m$ where a is the junction gradient, m is the grading coefficient, and x is the

TABLE 3.1. TURGEON-MATHEWS MODEL PARAMETERS

Primary Equations		
Description	Symbol	Expression
Built-in Voltage	ϕ_e, ϕ_c	$V_t \ln(N_a N_d / n_i^2)$
Recombination Currents	$I_1, I_2, \eta, I_3, I_4, \eta, I_5, I_6$	best fit
Depletion Capacitances	C_{jeo}, C_{jco}	$\epsilon A / x_{jo}$
Grading Coefficient	m_e, m_c	$1/(2+n)$
Saturation Current	I_S	$D_n \mu_p \rho_s q^2 n_i^2 A_e$
Early Voltages	V_{AO}, V_{BO}	$A_e / (\mu_p \rho_s C_{jo})$
Knee Currents	I_{KF}, I_{KR}	$2qA_e D_n p_{co} / W_{bo}$
Base Transit Times	τ_{fo}, τ_{ro}	$(W_{bo}^2 N_b)/2D_n p_{eo}$
Base High Injection	h_{eo}, h_{co}	$(n_i / p_{eo})^2$
Collector High Injection	h_{dc}	$(n_i / N_{dc})^2$
Unmodulated Collector Resistance	R_M	$\rho W_c / A_e$
Collector Charge	Q_{co}	$\tau_{co} I_D^2 / I_S$
Extrinsic Resistances	R_e, R_b, R_c	$\rho l / A$
Auxiliary Equations		
Zero-bias Depletion Width	x_{jo}	$\left[\frac{\epsilon_s \phi}{2 m_j q a} \right]^{m_j}$
Collector Diffusion Current	I_D	$q A_e N_{dc} \sqrt{D_n / \tau_{co}}$
Base Under Emitter Sheet Resistance	ρ_s	$1/q \mu_p N_b W_{bo}$

distance from the junction. In the GP model, ϕ_e and ϕ_c are determined by fitting to the C-V data and can differ significantly from the built-in potential calculated by $V_t \ln (N_a N_d / n_i^2)$.

The Early Voltages, for the one-dimensional modeling considered so far, are related to the depletion capacitances by Q_{bo}. To correct for the two-dimensional effects of the base-collector junction, independent parameters for the Early Voltages and depletion capacitances can be used. Because the area associated with base-emitter and base-collector junctions are not the same, C_{jco} is scaled by the ratio of the collector-base junction area to the emitter area. The knee currents are related to the transit times by Q_{bo} for one-dimensional modeling. To account for two-dimensional effects, the parameters can be chosen independently.

The parameters h_{eo}, h_{co}, and h_{dc} determine the onset of high injection at the base side of the emitter-base junction, the base side of the base-collector junction, and the collector side of the base-collector junction, respectively. R_M is the unmodulated epitaxial collector resistance and controls the onset of quasi-saturation. The amount of charge stored in the collector is controlled by the parameter Q_{co}. R_e, R_b, and R_c are the extrinsic emitter, base, and collector resistances. R_c corresponds to the resistance of the buried layer plus the resistance from the buried layer up to, and including, the collector contact. (R_c equals the sum of R_{bL} and R_{dc} of Figure 3.1a.)

Because the majority of the parameters can be extracted from the doping profile and geometry of the device, the model can be used to predict the transistor characteristics as a result of changes in the process and geometry. Thus, the circuit designer can observe how the transistor characteristics degrade with worst-case process variations and can keep these results in mind as he goes through the design process. Further, the predictive capabilities of the model can be used to enhance the characteristics by indicating to the device designer the effects of changing the doping profile . Given a set of

transistor characteristics. the typical modeling approach (given the doping profile and geometry of the device. use the model to predict the characteristics) can be reversed so that the model is used to obtain a set of parameters that fit the characteristics from which a doping profile corresponding to the model parameters can be determined.

CHAPTER 4

RESULTS

4.1. INTRODUCTION

This chapter contains the results of the performance of the GP and TM models. The fitting of the models to the dc characteristics of a shallow-base, high-voltage device is illustrated. The time required to evaluate each model in a dc analysis is compared. A number of conclusions regarding the tradeoffs between the accuracy and speed of the models are drawn and suggestions for future work are outlined. The "C" program functions from BIASC corresponding to the GP and TM models are contained in Appendices G and H, respectively.

4.2. ACCURACY

A shallow-base, high-voltage device was chosen to aid in observing some of the limitations associated with accurate modeling. The device has two emitters, each of size 4 μ by 50 μ. The I_C vs V_{ce}, β vs log I_C, and β vs I_C (high current) characteristics of the device are shown in Figure 4.1, Figure 4.2, and Figure 4.3, respectively. High-voltage devices have thick and lightly doped epitaxial layers which result in pronounced quasi-saturation effects. Turgeon and Mathews demonstrate the capability of their model for quasi-saturation in [Tur80]. Shallow-base devices have very narrow metallurgical basewidths (on the order of .1 - .2μ). It is important to be able to represent accurately the basewidth modulation and high-injection effects of these devices because, due to the small basewidth, they both have a significant impact on the total majority base charge.

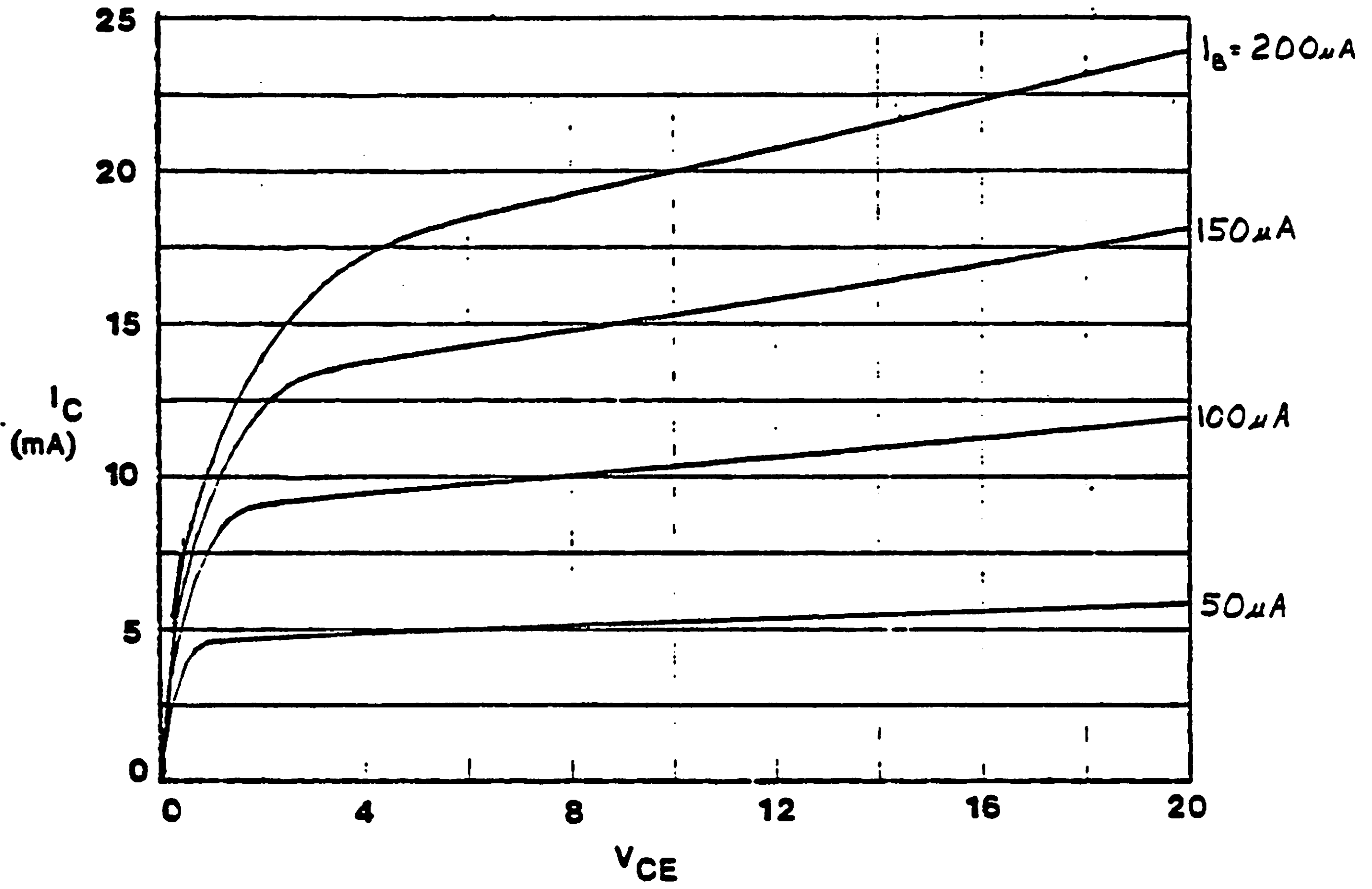

Figure 4.1. Common-Emitter Characteristics for a Shallow-Base, High-Voltage Device

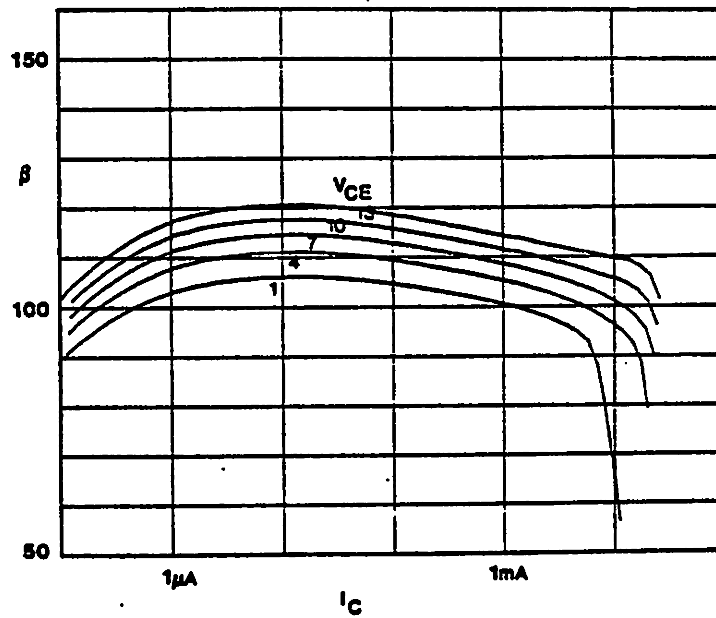

Figure 4.2. Output Characteristics for the Shallow-Base, High-Voltage Device

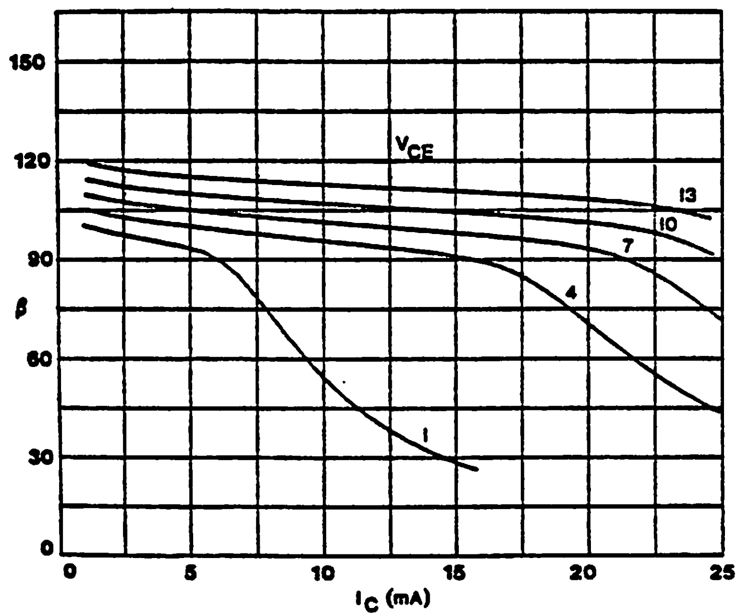

Figure 4.3 High Current Output Characteristics

4.2.1. The Gummel-Poon Model

The model parameters used for the GP model were provided by the manufacturer of the device. The resulting I_C vs V_{ce}, β vs log I_C, and β vs I_C (high current) curves are shown as solid lines in Figure 4.4, Figure 4.5, and Figure 4.6, respectively. The points in Figure 4.4 are data points from Figure 4.1. The parameters were measured corresponding to the techniques described in [Get76]. The IKF, ISE, NE, and R_c parameters were chosen to give a good fit at the edge of quasi-saturation. As noted by Getreu, since the GP model uses a constant collector resistance, the selection of R_c depends on what aspect of the device behavior is being modeled. Figure 4.4 illustrates the compromise of choosing R_c to be between its saturated and normal, active region value. The lack of quasi-saturation modeling is seen in the poor fit at low V_{ce} of Figure 4.4 and in the abrupt drop-off of β in Figures 4.5 and 4.6 that occurs when the model reaches saturation. The result of the Early voltage expression is seen in Figure 4.4 as the slope of the curves in the active region remain about the same for the GP output while in the measured curves of Figure 4.1 show that the slope (output conductance) increases with base current. The lack of a good fit over a large current and voltage range with this set of parameters is exhibited in the β vs log I_C curve of Figure 4.5.

4.2.2. The Turgeon-Mathews Model

A fit using the TM model for the I_C vs V_{ce}, β vs log I_C, and β vs I_C (high current) curves are shown as solid lines in Figure 4.7, Figure 4.8, and Figure 4.9, respectively. The points in Figure 4.7 are data points from Figure 4.1. Because of the very shallow junctions, the doping profiles of shallow-base devices are hard to determine and make it difficult to get accurate values for the TM parameters directly. With the use of a doping profile produced by SUPREM [Ant78], a first-order approximation

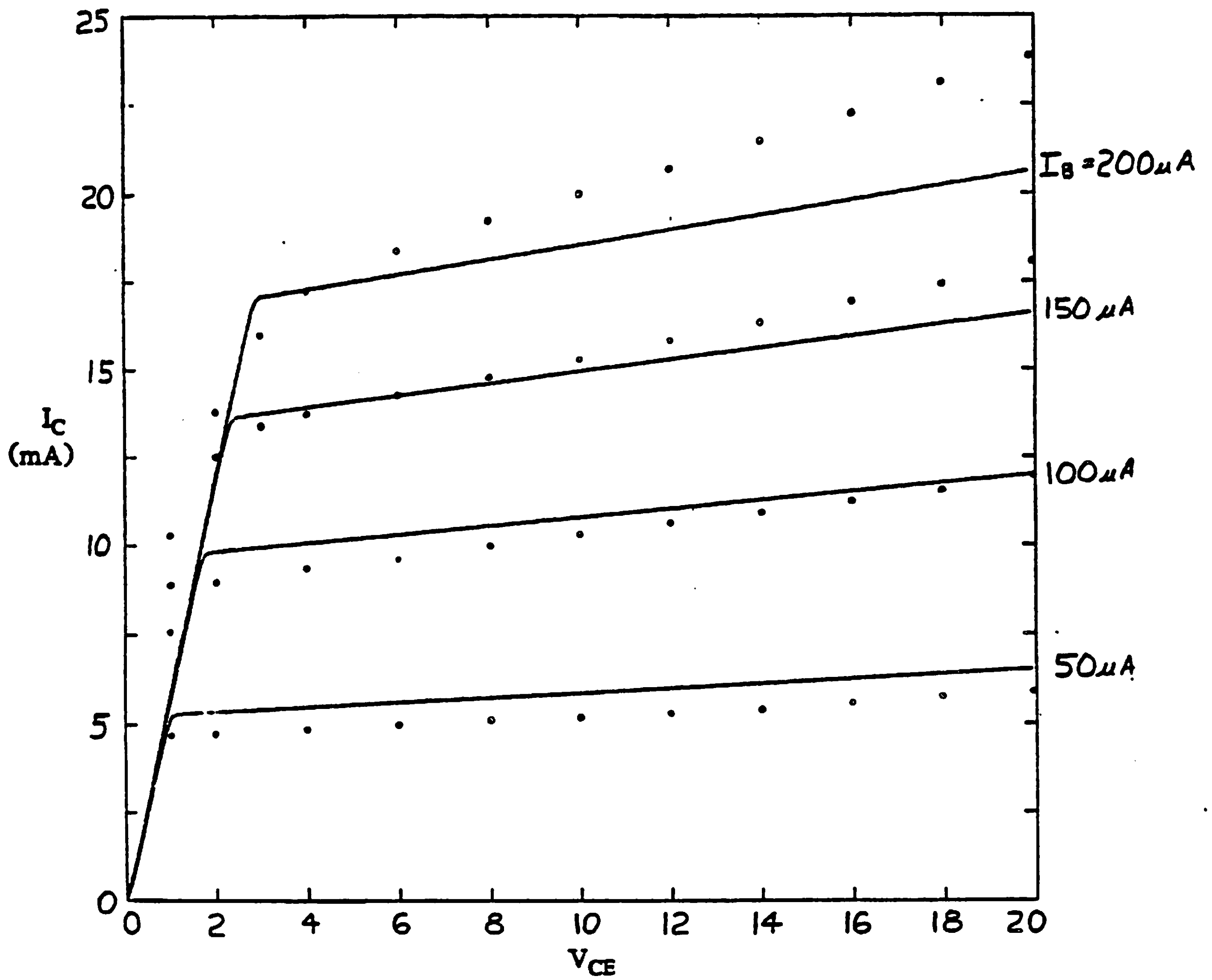

Figure 4.4. Common-Emitter Characteristics Using the Gummel-Poon Model

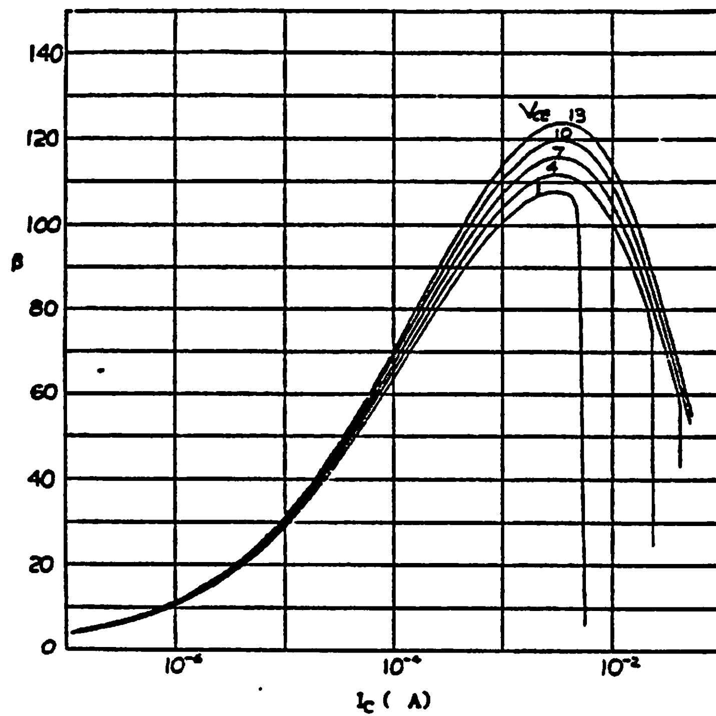

Figure 4.5. Output Characteristics Using the Gummel-Poon Model

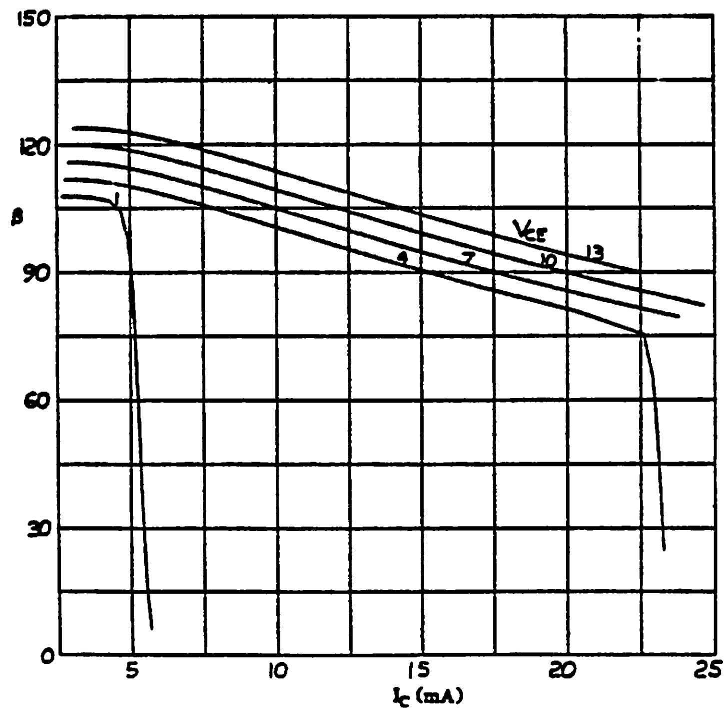

Figure 4.6. High Current Output Characteristics Using the Gummel-Poon Model

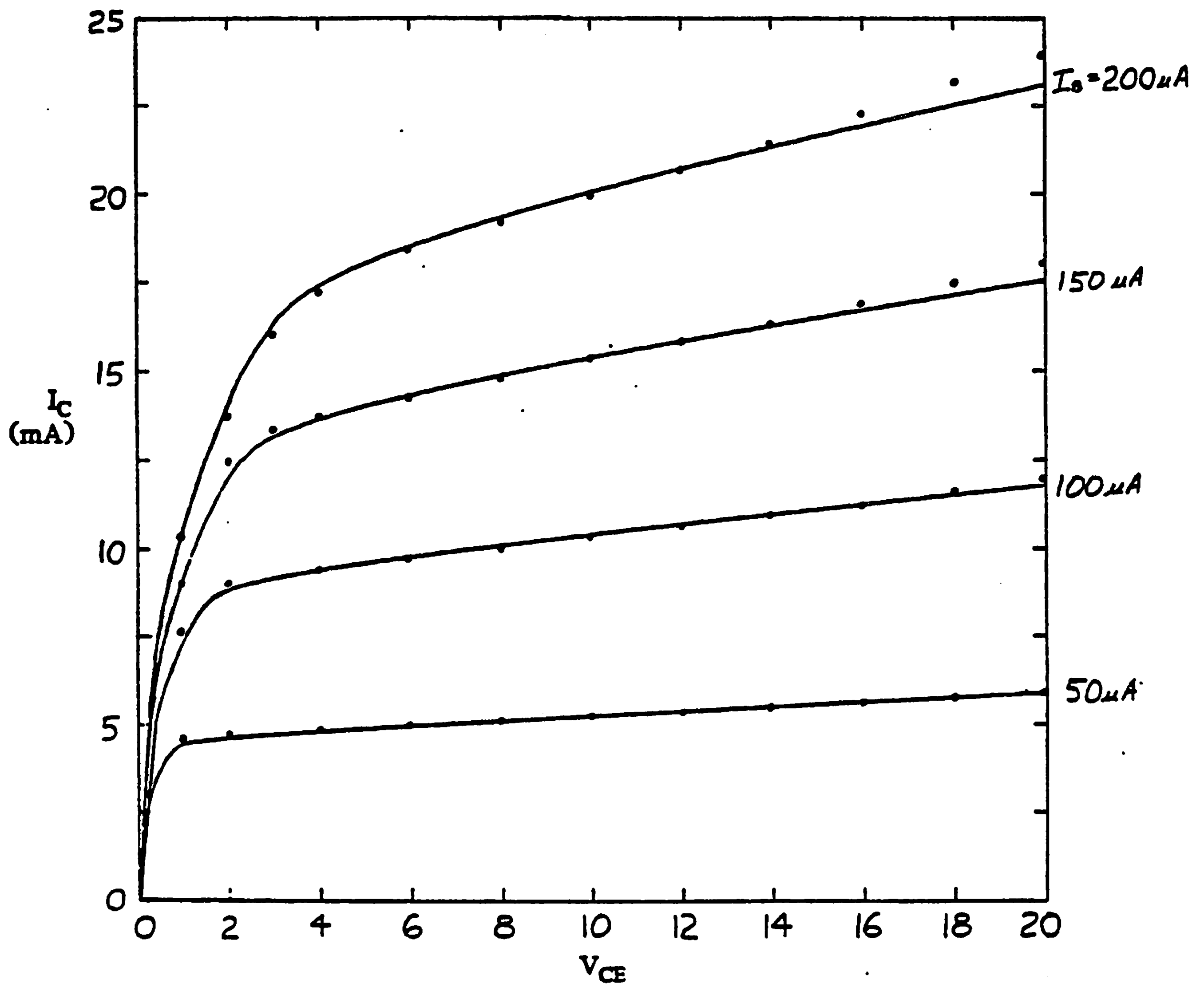

Figure 4.7. Common-Emitter Characteristics Using the Turgeon-Mathews Model

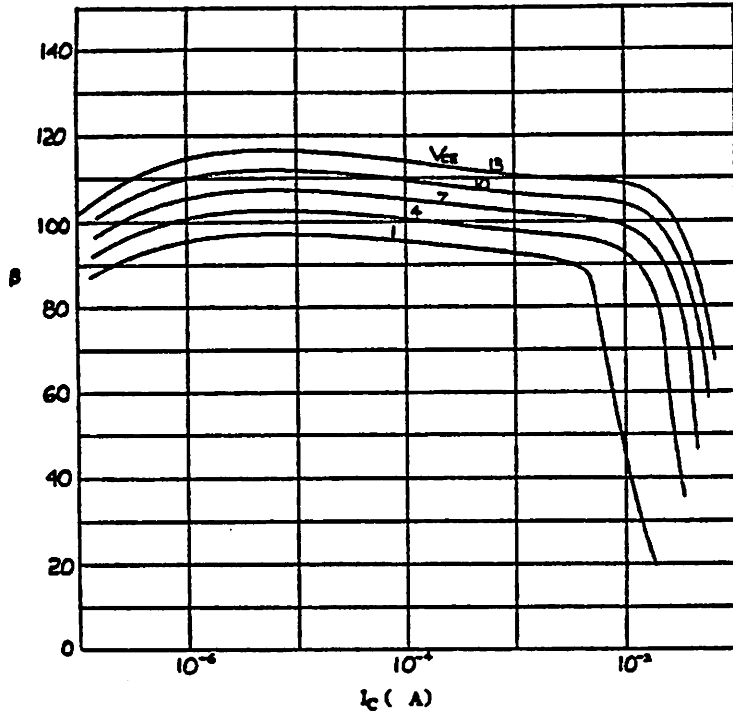

Figure 4.8. Output Characteristics Using the Turgeon-Mathews Model

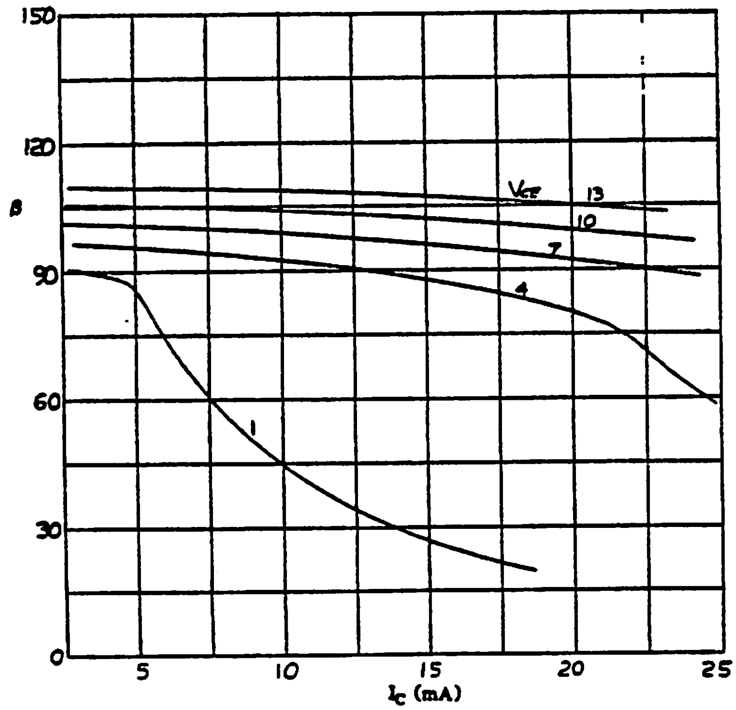

Figure 4.9. High Current Output Characteristics Using the Turgeon-Mathews Model

for most of the parameters is made according to the relationships of Table 3.1. I_S, I_1, I_2, and n_e are determined from a plot of $\ln(I_C)$ and $\ln(I_B)$ vs V_{be} with $V_{bc} = 0$. These parameters were further optimized V_{AO}, V_{BO}, m_e, m_c, h_{eo}, and I_{KF} are optimized by fitting to the I_C vs V_{ce} curve while also providing a reasonable fit to the β vs log I_C curve. I_5 and I_6 are chosen to give a good fit to the quasi-saturation region of the I_C vs V_{ce} curve. These figures show the ability of the TM model to fit over a large range of current and voltage biases. The fit shown in Figures 4.7, 4.8, and 4.9 can be improved upon with the use of optimization techniques.

4.3. SPEED OF EVALUATION

To determine the time spent in the model evaluation, a dc transfer analysis of the I_C vs V_{ce} characteristics was performed. Table 4.1 lists the typical model evaluation times for the GP and TM models. The numbers apply to a single evaluation of each model.

Model	Typ. Eval. Time (ms)	Rel. Eval. Time
GP	1.35	1.0
TM	2.13	1.6

Table 4.1 Evaluation Times for the Models

The column in Table 4.1 labeled "Relative Evaluation Time" indicates the cost involved for the TM model over the GP model. The TM model requires 60% more time than the GP model for the dc analysis using BIASC. A major portion of this increased cost is due to an increase in the number of expensive expressions, the exponential, power, and logarithmic functions, that must be evaluated. In the GP model for dc analysis, four exponential calculations (the base current terms), two logarithmic calculations (the expressions used in limiting the junction voltage for convergence purposes), and a square root calculation (the base charge term) are performed.

The TM model contains seven exponential expressions (the same four as the GP model, and the g_e, g_c, and R_{ci} terms), three power expressions (the depletion charges q_{de} and q_{dc} and the current-crowding term A_e'), and a logarithmic expression (the I_{bcc} term) that are evaluated. For the TM model, approximately 41% of the model evaluation time was spent evaluating these more costly functions while in the GP model the corresponding proportion of time was 61%.

4.4. CONCLUSIONS

The results of Sections 4.2 and 4.3 indicate that there is a tradeoff between the accuracy and evaluation time of models. The TM model provides a more accurate fit to the dc characteristics than the GP model while requiring a longer model evaluation time due mainly to the addition of high-injection and quasi-saturation terms. An important point to note regarding the model evaluation time for dynamic analyses is that the GP will have to evaluate two power expressions for the depletion charges while the TM model will not incur any additional expensive functions. Thus, the difference in relative evaluation times between the two models will decrease.

One difficulty encountered with the TM model for shallow-base devices is in determining the parameters from the doping profile. Because the doping gradients are large and the location of the depletion edges are hard to determine in these devices, only approximate values for many of the parameters can be obtained. Then, the parameters can be optimized to provide better agreement with the measured characteristics.

4.5. FUTURE WORK

To compare more completely the capabilities of the GP and TM models, the model parameters should be optimized using some sort of general optimizer to give as good a

fit as possible to the transistor characteristics. This will indicate the robustness (with respect to accuracy) of the models. If the values of some parameters become physically unreasonable, then the equations using these parameters may not be accurate for the transistor under consideration. Further, experiments comparing the dynamic capabilities should be performed to investigate if the TM model results in more accurate transient and ac analyses than the GP model. This will involve comparing the capabilities of the models to fit to the f_T vs I_C characteristics and how accurately the models predict the response to pulsed inputs. These experiments should be conducted on several devices of different profiles and processes to verify the accuracy of the TM model and to recognize better the capabilities and limitations of the model.

As CAD (computer-aided-design) progresses, the need for robust models increases so that the person using the design tools does not have to choose an appropriate model depending on what the current, voltage, or frequency range of operation is. Preferably, a model can be used that is adequate over as large of a region of operation as possible while incurring an evaluation time that is not prohibitive. With the development of implementing models in hardware [Gyu85], the tradeoff between accuracy and evaluation time may shift in the direction of desiring additional accuracy while sacrificing some of the speed improvements.

There are several limitations of the bipolar models that are not addressed in this report. As the basewidths are reduced, the collector-base space-charge transit time becomes increasingly important and can dominate the total transit time [Mey86]. To obtain an accurate expression for this transit time, the scattering-limited velocity of carriers traversing the collector-base space-charge region must be incorporated into the bipolar model. This is not done in either the GP or TM models. Another property not accounted for in either model is the reduction of the epitaxial resistance as the collector-base depletion region widens with increasing reverse bias while the transistor

is in the forward active region of operation [Mac82]. Additional limitations are encountered with the two- and three-dimensional nature of the device, some of which become more critical as the length and width of the emitter is scaled down [Lac82]. The distributed nature of the base-collector junction has resulted in the use of a split of the junction capacitance between an external and internal capacitance and the use of a base resistance that incorporates a classical analysis of current crowding [Hau64]. Both of these approximations can provide improvements, but in practice the extrinsic base-collector region is usually modeled as a combination of diodes and resistors. As the area of the devices are progressively reduced, the adequacy of one-dimensional analysis becomes further restricted [Kne85] and the need for a device simulator to interact in the design environment (a mixed-mode simulator [Eng82] is an example) becomes increasingly important [Lac82]. The achievement of smaller devices has been aided by using polysilicon to connect to the emitter, base, and collector of the transistor. The polysilicon-to-silicon interface is not fully understood and results in some undesirable and sometimes unpredictable properties for resistance and junction capacitance. Investigating this interface further can allow the designing of more optimal devices and provide improvements in the model.

APPENDIX A: EPITAXIAL COLLECTOR RESISTANCE MODULATION

An expression for the collector epitaxial resistance modulation is derived by solving the basic current transport equations subject to boundary conditions as illustrated in Fig.3.3.The voltage difference from $x = 0$ to $x = W_c$ is obtained by integrating the electric field in that region.

$$V_c = \int_0^{x_1} E dx + \int_{x_1}^{W_c} E dx \tag{A.1}$$

The electric field, E, in the conductivity modulated portion of equation (A.1) ($0 \le x \le x_1$) is replaced using the following small difference approximation.

$$J_p << q \mu_p p_n E \approx q D_p \frac{\partial p_n}{\partial x} \tag{A.2}$$

The expression for the voltage across the collector epi region becomes

$$V_c = V_t B + \frac{J_n W_c}{q \mu_n N_{dc}} \left(1 - \frac{x_1}{W_c}\right) \tag{A.3}$$

where Ohm's law ($J_n = q \mu_n N_{dc} E$) was substituted in for the constant electric field in the drift region. The "B" is defined as follows:

$$B = \int_0^{x_1} \frac{1}{p_n} \frac{\partial p_n}{\partial x} dx \tag{A.4}$$

Equation (A.4) need not be evaluated further, because it will be shown that it cancels by defining a position x_0 that replaces x_1 such that the total collector resistance is modeled by an effectively equivalent ohmic resistance. The effective resistance across the epitaxial region is obtained by dividing equation (A.3) by the collector current density.

$$R_{ci} = \frac{V_c}{A_e J_n} = R_M \left(1 - \frac{x_1}{W_c}\right) + \frac{V_t B}{A_e J_n} \tag{A.5}$$

where $R_M = W_c / q \mu_n N_{dc} A_e$ is the maximum epitaxial collector resistance.

The normalized position x_1/W_c is derived from the electron current density equation as follows:

$$J_n = q\mu_n n_n E + qD_n \frac{\partial n_n}{\partial x} = \frac{qD_n}{p_n}\left(n_n \frac{\partial p_n}{\partial x} + p_n \frac{\partial n_n}{\partial x}\right)$$

$$= qD_n \left(\frac{n_{no} + p_{no} + 2\Delta p_n}{p_n}\right)\frac{\partial p_n}{\partial x} \tag{A.7}$$

where the electric field, E, in equation (A.7), was replaced using equation (A.2). This is a reasonable approximation because the hole current density, J_p, is controlled by a small difference between the drift and diffusion currents in the conductivity modulated region. Furthermore, the total charge carriers were divided into an unbiased level n_{no}, p_{no} and an excess level Δp_n at the junction edge (i.e. $n_n = n_{no} + \Delta p_n$ and $p_n = p_{no} + \Delta p_n$), and quasi-neutrality (i.e. $\Delta p_n \approx \Delta n_n$) was assumed.

Integrating both sides of equation (A.7), and using the approximations $p_n \approx \Delta p_n$ and $n_{no} \approx N_{dc} >> p_{no}$ results in the following:

$$\int_0^{x_1} \frac{J_n}{qD_n} dx = \int_0^{x_1} 2\frac{\partial p_n}{\partial x} dx + \int_0^{x_1}\left(\frac{n_{no} + p_{no}}{p_n}\right)\frac{\partial p_n}{\partial x} dx \tag{A.8}$$

$$\frac{J_n x_1}{qD_n} = 2\,(p_{x_1} - p_0) + N_{dc} B \tag{A.9}$$

Furthermore, by defining conductivity modulation to be significant when the injected carriers exceed half of the epitaxial doping (i.e. $p_{x_1} = N_{dc}/2$), the following expression results.

$$\frac{x_1}{W_c} = \frac{qD_n N_{dc}}{W_c J_n}\left(1 - 2\frac{p_0}{N_{dc}}\right) + \frac{qD_n N_{dc} B}{J_n W_c}$$

$$= \frac{V_t}{I_{cc} R_M}\left(1 - 2\frac{p_0}{N_{dc}}\right) + \frac{V_t B}{R_M I_{cc}} \tag{A.10}$$

Substituting equation (A.10) into equation (A.5) cancels the "B" terms (i.e. eq. (A.4)) and the resulting collector resistance expression is.

$$R_{ci} = R_M\left(1 - \frac{x_0}{W_c}\right) \tag{A.11}$$

Furthermore, the normalized distance x_0/W_c is defined as:

$$\frac{x_0}{W_c} = \frac{V_t}{I_{cc}R_M}\left(2\frac{p_0}{N_{dc}} - 1\right) \tag{A.12}$$

and the minority carrier injection level at the edge of the base collector junction is given by:

$$\frac{p_0}{N_{dc}} = \left(\frac{n_i}{N_{dc}}\right)^2 (e^{V_{bci}/V_t} - 1)g_c \tag{A.13}$$

where the function $g_c \equiv g(V_{bci})$ is defined in Appendix D. Equations (A.11), (A.12), (A.13) form the collector resistance modulation model of the bipolar transistor.

Since the transport current, I_{cc} is in the denominator of equation (A.12), it can be a problem if it is allowed to have a zero value. The singularity can be avoided† by simply forcing a lower bound on I_{cc} (i.e. I_{ccm}). Holding I_{cc} independent of bias for $I_{cc} < I_{ccm}$ not only avoids the discontinuity, but establishes the inverse gain of the transistor model when $I_{cc} < 0$.

APPENDIX B: RECOMBINATION CURRENT IN THE COLLECTOR REGION

The recombination current expression in the collector epitaxial region takes into account the carrier lifetime dependence on carrier injection level by using the following carrier lifetime model.

$$\tau = \frac{\tau_c}{\tau_{c0}} = \frac{N_{dc} + \tau_r \Delta p_n}{N_{dc} + \Delta p_n} \tag{B.1}$$

The model depends on the epitaxial layer doping, N_{dc}, the excess minority carrier injection, Δp_n, and the ratio of the lifetime at low level, τ_{c0}, and high level, τ_{∞}, injection (i.e. $\tau_r \equiv \tau_{\infty}/\tau_{c0}$). Note, that for $\tau_r = 1$ the lifetime is independent of the injection level. Furthermore, for $\tau_r > 1$ the lifetime becomes longer with injection level and for $\tau_r < 1$ the lifetime shortens with injection level. For our processes, we have found that the lifetime ratio is about ten percent (i.e. $\tau_r \approx 0.1$).

---

† If we adhered to the exact limit when integrating equation (A.8), the numerator of equation (A.12) would equal zero whenever I_{cc} is equal to zero. This condition justifies the selection of a lower bound for I_{cc}.

The collector region recombination current, I_{bcc}, is derived by integrating the ratio of hole concentration to lifetime in the epitaxial layer.

$$I_{bcc} = qA_e \int_0^{W_e} \frac{p_n}{\tau_c} dx \tag{B.2}$$

Substituting equation (B.1) for τ_c, and performing a change of variable from "x" to "p_n" results in:

$$I_{bcc} = \frac{qA_e}{\tau_{c0}} \int_{p_0}^{p_{W_e}} \frac{p_n}{\left(\dfrac{N_{dc} + \tau_r p_n}{N_{dc} + p_n}\right)} \frac{dp_n}{\left(\dfrac{\partial p_n}{\partial x}\right)} \tag{B.3}$$

Furthermore, replacing the $\dfrac{\partial p_n}{\partial x}$ term by equation (A.8) and assuming $N_{dc} \approx n_{no} + p_{no}$ and $\Delta p_n \approx p_n$ the following form of I_{bcc} is obtained:

$$I_{bcc} = \frac{q^2 A_e D_n}{\tau_{c0} J_n} \int_{p_0}^{p_{W_e}} \frac{(N_{dc} + p_n)(N_{dc} + 2p_n)}{N_{dc} + \tau_r p_n} dp_n$$

$$= \frac{q^2 D_n N_{dc}{}^2 A_e{}^2}{\tau_{c0} I_{cc}} \int_{\frac{p_0}{N_{dc}}}^{\frac{p_{W_e}}{N_{dc}}} \frac{1 + 3p_n' + 2p_n'^2}{1 + \tau_r p_n'} dp_n' \tag{B.4}$$

where p_n' is the normalized excess hole concentration define as $p_n' = p_n / N_{dc}$. Since the excess minority carrier concentration decreases with increasing distance away from the base-collector junction it is correct to have $W_c \rightarrow \infty$ which results in $P_{W_e}/N_{dc} \rightarrow 0$ and simplifies the integration of equation (B.4).

Integrating equation (B.4) and evaluating at the limits results in the following collector recombination current:

$$I_{bcc} = \frac{I_D{}^2}{I_{cc}\tau_r} \left[\left(1 - \frac{3}{\tau_r} + \frac{2}{\tau_r{}^2}\right) \ln\left(\tau_r \frac{p_0}{N_{dc}} + 1\right) + \left(3 - \frac{2}{\tau_r}\right) \frac{p_0}{N_{dc}} + \left(\frac{p_0}{N_{dc}}\right)^2 \right] \tag{B.5}$$

where $I_D{}^2 = q^2 D_n N_{dc}{}^2 A_e{}^2 / \tau_{c0}$ is a bias voltage independent parameter.

APPENDIX C: COLLECTOR REGION STORED CHARGE

The stored diffusion charge in the epitaxial collector region is calculated by integrating the minority carrier charge density as follows:

$$Q_c = qA_e \int_0^{W_e} p_n dx$$
$$= qA_e \int_{p_0}^{p_{W_e}} p_n \frac{dp_n}{\left(\frac{\partial p_n}{\partial x}\right)} \tag{C.1}$$

Substituting equation (A.7) into equation (C.1) results in:

$$Q_c = q^2 D_n A_e \int_{p_0}^{p_{W_e}} \frac{(N_{dc} + 2p_n)}{J_n} dp_n$$
$$= \frac{q^2 D_n A_e^2 N_{dc}^2}{I_{cc}} \left[\frac{p_0}{N_{dc}} + \left(\frac{p_0}{N_{dc}}\right)^2\right]$$
$$= \frac{\tau_{c0} I_D^2}{I_{cc}} \left[\frac{p_0}{N_{dc}} + \left(\frac{p_0}{N_{dc}}\right)^2\right] \tag{C.2}$$

Equation (C.2) represents the stored charge in the collector epitaxial region for a given injection level (determined by p_0/N_{dc} from equation (A.13)) and base transport current, I_{cc}. Note that for $\tau_r = 1$ the stored charge in the collector is related to the collector recombination current as follows:

$$Q_c = I_{bcc} \tau_{c0} \tag{C.3}$$

That is, if the lifetime is independent of the injection level, the recombination current and stored charge are related by lifetime only.

APPENDIX D: PN JUNCTION EXPRESSION FOR HIGH INJECTION

The modeling of the Early effects, the base transit times, and the transistor dynamics requires bias voltage dependent junction depletion edges. The classical solution of the Poisson equation in a pn junction yields a depletion width expression that approaches zero as the internal junction voltage approaches the junction built-in voltage. This depletion width behavior is inconsistent with the

classical injection expression that permits an infinite forward bias voltage. B. R. Chawla et al.[10] resolve this problem by empirically modifying the classical depletion capacitance expression to permit the junction voltage to exceed the built-in voltage. In contrast, we use a carrier injection expression that limits the internal junction voltage to be less than the built in voltage. Even though this concept has been previously considered by other authors such as S. M. Sze[11], N. H. Fletcher[12] and S. R. Dhariwal[13], we present a short novel derivation, in this Appendix, that clarifies the physics and establishes the validity of the model.

The carrier concentration on either side of a pn junction can be expressed as:

$$n_p = n_n \, e^{(V_j - \phi)/V_t} \tag{D.1}$$

where the internal junction potential variation is defined as $V_j \equiv \phi - (\psi_n - \psi_p)$. The subscripts "p" and "n" refer to the p and n sides of the pn junction respectively. The law of the junction for high injection is obtained by evaluating the excess minority carrier concentration on the p side of the junction, while retaining the excess majority carrier concentration, Δn_n as follows.

$$\begin{aligned}
\Delta n_p = n_p - n_{p0} &= n_n \, e^{(V_j - \phi)/V_t} - n_{p0} \\
&= (\Delta n_n + n_{n0}) \, e^{(V_j - \phi)/V_t} - n_{p0} \\
&= \Delta n_n \, e^{(V_j - \phi)/V_t} + n_{n0} \, e^{(V_j - \phi)/V_t} - n_{p0} \\
&= \Delta n_n \, e^{(V_j - \phi)/V_t} + n_{p0} \, e^{(\phi/V_t)} e^{(V_j - \phi)/V_t} - n_{p0} \\
&= \Delta n_n \, e^{(V_j - \phi)/V_t} + n_{p0} \, (e^{V_j/V_t} - 1)
\end{aligned} \tag{D.2}$$

Using the quasi-neutrality and symmetry approximations $\Delta n_n = \Delta n_p$, (which improves under forward bias conditions) the following excess minority carrier concentration results.

$$\Delta n_p = n_{p0} \frac{e^{V_j/V_t} - 1}{1 - e^{(V_j - \phi)/V_t}} \tag{D.3}$$

Note, that if the excess majority carriers, Δn_n, are neglected in equation (D.2), equation (D.3) reduces to the classical low injection law.

Using equation (D.3), the current for a pn junction diode can be expressed as:

$$I_j = I_{j0}(e^{V_j/V_t} - 1)\, g(V_j) \tag{D.4}$$

where I_{j0} is the reverse leakage current. The function $g(V_j)$ represents a high injection correction factor to the classical junction law that we defined as:

$$g(V_j) = \frac{1}{1 - e^{(V_j - \phi)/V_t}} \tag{D.5}$$

Equation (D.5) takes into account the built-in voltage in the pn junction law. This is important for high injection modeling, because without this correction factor the internal bias on the junction is unrestricted and can exceed the built-in voltage, which results in unphysical behavior.

Furthermore the spatial location of the excess carrier concentration must be known to fully define the boundary condition. The classical solution of Poisson's equation yields the following junction depletion edge definition:

$$x_j = x_{j0}\left(1 - \frac{V_j}{\phi}\right)^{m_j} \tag{D.6}$$

where ϕ and m_j are the built-in voltage and grading coefficient respectively. Our high injection model (D.3) avoids the discontinuity in equation (D.6) by constraining the internal junction voltage to be less than the built-in voltage (i.e. $V_j \leq \phi$). Under high injection conditions the depletion width approaches zero and the current becomes unlimited by the pn junction (i.e. the pn junction becomes a short circuit). For pn junction diodes, the current is limited by the resistance in series with the pn junction.

APPENDIX E : BASE TRANSPORT CURRENT

Using the small difference approximation, $E \approx \frac{V_t}{p}\frac{dp}{dx}$, and the Einstein relationship, $\mu_n = D_n/V_t$, in the electron current density expression yields the following relationship.

$$J_n = q\mu_n nE + qD_n \frac{dn}{dx} = \frac{qD_n}{p}\frac{d(np)}{dx} \qquad \text{(E.1)}$$

Integrating both sides of equation (E.1) from the base side of the base-emitter junction, x_e, to the base side of the base-collector junctions, x_c, results in the following base transport current expression.

$$I_{cc} = -A_e J_n = \frac{qD_n A_e (n_e p_e - n_c p_c)}{\int_{x_e}^{x_c} p\, dx} \qquad \text{(E.2)}$$

The $n_e p_e$ and $n_c p_c$ terms are the electron and hole products at the bias voltage dependent boundaries x_e and x_c respectively. Except for the location of the boundaries x_e and x_c, equation (E.2) is the standard base transport equation found in the literature[14] [15].

The numerator of equation (E.2) is evaluated by separating the electron-hole products ($n_e p_e$ or $n_c p_c$) into the sum of a zero bias and an excess term, $n_e p_e = (\Delta n_e + n_{e0})(\Delta p_e + p_{e0})$, and substituting Δn_e and Δp_e from equation (D.3).

$$n_e p_e = p_{e0} n_{e0} \left[\frac{e^{V_{bei}/V_t} - 1}{1 - e^{(V_{bei} - \phi_b)/V_t}} + 1 \right] \left(1 + \frac{\Delta p_e}{p_{e0}} \right)$$

$$= n_i^2 e^{V_{bei}/V_t} g_e h_e \qquad \text{(E.3)}$$

The condition $e^{-\phi/V_t} << 1$ was used, and $g_e \equiv g(V_{bei})$ is given in Appendix D. Furthermore, h_e is defined as follows:

$$h_e \equiv h(V_{bei}) = 1 + \frac{\Delta p_e}{p_{e0}} = 1 + h_{e0} e^{V_{bei}/V_t} g_e \qquad \text{(E.4)}$$

where $h_{e0} \equiv \left(\frac{n_i}{p_{e0}} \right)^2$. Equation (E.4) models high injection in the base region. The resulting transport equation (E.2) then becomes:

$$I_{cc} = I_s \frac{e^{V_{bei}/V_t} g_e h_e - e^{V_{bci}/V_t} g_c h_c}{q_b(V_{bei}, V_{bci})} \qquad \text{(E.5)}$$

where $I_s \equiv q^2 A_e^2 D_n n_i^2 / Q_{b0}$ and $Q_{b0} \equiv qA_e \int_{x_{e0}}^{x_{c0}} p dx = qA_e N_b W_{b0}$. The term Q_{b0}

represents the total majority carrier concentration in the base under zero bias conditions and N_b represents the average base doping under zero bias conditions.

The denominator of equation (E.5) is the normalized majority carrier concentration, which when integrated can be expressed as follows:

$$q_b(V_{bei},V_{bci}) = \frac{1}{Q_{b0}}\int_{x_e}^{x_c} p\,dx = 1 + \frac{Q_{je} + Q_{jc} + Q_{de} + Q_{dc}}{Q_{b0}} \qquad \text{(E.6)}$$

The Q_{je} and Q_{jc} are the depletion charges, which represent the change from zero bias of ionized donor-electron or acceptor-hole pairs, while Q_{de} and Q_{dc} are the base diffusion charges terms representing the change in free electron-hole pairs from zero bias, both of which depend on V_{bei} and V_{bci}.

The depletion charges, when integrated from x_{e0} to x_e and x_{c0} to x_c, result in the classical depletion capacitance charge expression (equation 3.8).The change in diffusion charge is obtained by approximating the integral, of the excess free electron-hole pairs in the denominator of equation (E.2), by a trapezoid from x_e to x_c, and assuming that $\Delta n_e \approx \Delta p_e$ in the base region.

$$Q_d = Q_{de} + Q_{dc} = qA_e\left(\frac{\Delta n_e + \Delta n_c}{2}\right)\left(W_{b0} + \Delta x_{je} + \Delta x_{jc}\right) \qquad \text{(E.7)}$$

The terms Δx_{je} and Δx_{jc} are the change in depletion width of the junctions, which are equal to zero at zero bias. W_{b0} is the depletion edge zero bias base width. Δn_e and Δn_c are the injected excess electron concentrations at the emitter and collector junction edges inside the base region, which are also defined to be zero under zero bias.

Using the expressions for the excess minority concentration Δn_e derived in appendix D, Q_{de} can be expressed as follows:

$$
\begin{aligned}
\frac{Q_{de}}{Q_{b0}} &= \frac{qA_e \Delta n_e W_{b0}}{2Q_{b0}} \left(1 + \frac{\Delta x_{je} + \Delta x_{jc}}{W_{b0}}\right) \\
&= \frac{qA_e W_{b0} n_i^2 (e^{V_{bei}/V_t} - 1) g_e f_e}{2Q_{b0} a_e x_{je0}} \\
&= \frac{I_s}{I_{KF}} (e^{V_{bei}/V_t} - 1) g_e f_e
\end{aligned}
\qquad \text{(E.8)}
$$

where $I_{KF} = 2qA_e D_n p_{e0}/W_{b0}$ is the forward knee current and f_e is given as follows:

$$
\begin{aligned}
f_e &= \frac{1 + \dfrac{\Delta x_{je} + \Delta x_{jc}}{W_{b0}}}{\left(1 - \dfrac{V_{bei}}{\phi_e}\right)^{m_e}} \\
&= \frac{1 + \dfrac{V_{B0}\left[1 - \left(1 - \dfrac{V_{bei}}{\phi_e}\right)^{m_e}\right] + V_{A0}\left[1 - \left(1 - \dfrac{V_{bci}}{\phi_c}\right)^{m_c}\right]}{2V_p}}{\left(1 - \dfrac{V_{bei}}{\phi_e}\right)^{m_e}}
\end{aligned}
\qquad \text{(E.9)}
$$

where $V_{A0} = Q_{b0} x_{jc0}/\epsilon A_e$ and $V_{B0} = Q_{b0} x_{je0}/\epsilon A_e$ are the forward and reverse Early voltage parameters and $V_p = Q_{b0} W_{b0}/\epsilon A_e$ is related to the "punch through" voltage. The symbol "ϵ" represents the permittivity of silicon. Ignoring the emitter-junction depletion width change, the punch through voltage is approximately equal to:

$$
V_{pt} = \phi_c \left[1 - \left(1 - \frac{2V_p}{V_{A0}}\right)^{1/m_c}\right] \qquad \text{(E.10)}
$$

The punch-through condition occurs when $Q_{je} + Q_{jc} + Q_{b0} = 0$ and $f_e = f_c = 0$.

Base Transit Time:

Integrating the electron velocity in the base region ($J_n = qnv_n$) from the emitter-base depletion edge to the base-collector depletion edge results in:

$$t_b = \int_{x_e}^{x_c} \frac{dx}{v_n} = \frac{qA_e}{I_{cc}} \int_{x_e}^{x_c} n\, dx = \frac{Q_{de} + Q_{dc}}{I_F + I_R}$$

$$= \frac{t_f}{1 + I_R/I_F} + \frac{t_r}{1 + I_F/I_R} \qquad \text{(E.11)}$$

where $I_F = \dfrac{I_s e^{V_{bei}/V_t} g_e h_e}{q_b}$ and $I_R = \dfrac{I_s e^{V_{bci}/V_t} g_c h_c}{q_b}$ are the forward and reverse transport currents. The resulting forward and reverse transit time expressions are $t_f = \dfrac{Q_{de}}{I_F} = t_{f0}\dfrac{q_b f_e}{h_e}$, and $t_r = \dfrac{Q_{dc}}{I_R} = t_{r0}\dfrac{q_b f_c}{h_c}$.

The transit time parameters t_{f0} and t_{r0} (given in Table 3.1) are defined to be the limit of t_f and t_r as V_{bei} and V_{bci} approach zero. All of the parameters in this modeling are defined at zero bias conditions, resulting in a set of modeling parameters that are obtainable from the doping profile and transistor geometry.

APPENDIX F: LISTING OF THE GUMMEL-POON MODEL FUNCTION

```
/*
 *  This file, gp.c, contains the Gummel-Poon
 *  bipolar model evaluation.
 */
#include <math.h>
#include "types.h"
#include "extern.h"
#include "defs.h"
#define max(a,b) ((a) > (b) ? (a) : (b))
#define min(a,b) ((a) > (b) ? (b) : (a))
#define abs(a)   ((a) < 0.0 ? -(a) : (a))

extern double    abstol, reltol, vntol, trtol;
extern int          orinc;

gp(atype)
int atype;

{
        float is,gmf,gmr,icc,ice,vbe,ovbe,vbc,ovbc,vt,icn,gmin,gpi,gmu,type;
        float vcritbe, vcritbc, bf, br, gbl, gb, gc, ge;
        float icfn, icrn, ibl, ibln, ib2, ib2n, g1, g2, isc, ise, nc, ne;
        float vaf, var, ovaf, ovar, ikf, ikr, oikf, oikr, q1, q2, qb, sqarg;
        float gcbc, cjc,vjc,mjc,fc,arg,sarg,capbc,irhsbc;
        float gcbxc, capbxc, irhsbxc, vbxc, cjbxc, xcjc;
        float gcbe, gcbebc, cje,vje,mje,capbe,irhsbe;
        float gcsc, cjs,vjs,mjs,capsc,irhssc,vsc;
        float tr, tf, dqbdvbe, dqbdvbc, gm, go;
        float oic, oib, ic, ib, iccon, ibcon, delvbe, delvbc;
        float po, xowc, nd, rmax;
        float oldvbc;
        float pnjlim();
        double exp(), log(), sqrt();

        struct bjt *btemp;
        struct bjtimfo *bitemp;

        extern float vtherm, tstep, ni, nit;
        extern int nocon, tritct;
        extern struct bjt *bjt;

        gmin = fvalue("gmin");

        for (btemp = bjt; btemp; btemp = btemp->nextbjt) {
                bitemp = btemp->bim;

                rmax = btemp->bmptr->rmax/btemp->ae;
                gbl = btemp->ae/btemp->bmptr->rbl;
                gb = btemp->ae/btemp->bmptr->rb;
                ge = btemp->ae/btemp->bmptr->re;
                bf = btemp->bmptr->bf;
                br = btemp->bmptr->br;
                is = btemp->bmptr->is*btemp->ae;
                ise = btemp->bmptr->ise*btemp->ae;
                isc = btemp->bmptr->isc*btemp->ae;
                ne = btemp->bmptr->ne;
                nc = btemp->bmptr->nc;
                vaf = btemp->bmptr->vaf;
                var = btemp->bmptr->var;
                ikf = btemp->bmptr->ikf*btemp->ae;
                ikr = btemp->bmptr->ikr*btemp->ae;
                if(vaf==0)
                        ovaf=0.0;
                else
                        ovaf=1/vaf;
```

```
if(var==0)
        ovar=0.0;
else
        ovar=1/var;
if(ikf==0)
        oikf=0.0;
else
        oikf=1/ikf;
if(ikr==0)
        oikr=0.0;
else
        oikr=1/ikr;
vt = vtherm;
vcritbe = vt*log(vt/(1.414*is*(bf+1)/bf));
vcritbc = vt*log(vt/(1.414*is*(br+1)/br));
type = 1.0;    /* default to npn device */
if(!btemp->bmptr->btype) type = -1.0;    /* pnp device */

while(bitemp) {

        vbe = 0.0;
        vbc = 0.0;
        vbxc = 0.0;
        icc = 0.0;
        ice = 0.0;
        vsc = 0.0;

        if (bitemp->nbivalue) {
                vbe = type*bitemp->nbivalue->ovalue;
                vbc = vbe;
        }
        if (bitemp->nbxvalue)
                vbxc = type*bitemp->nbxvalue->ovalue;
        if (bitemp->neivalue) {
                vbe -= type*bitemp->neivalue->ovalue;
        }
        if (bitemp->ncivalue) {
                vbc -= type*bitemp->ncivalue->ovalue;
                vbxc -= type*bitemp->ncivalue->ovalue;
        }
        if (bitemp->ncnvalue)
                vsc -= type*bitemp->ncnvalue->ovalue;
        if (bitemp->nsvalue)
                vsc += type*bitemp->nsvalue->ovalue;

        ovbe = bitemp->ovbiei;
        ovbc = bitemp->ovbici;
        oic = bitemp->oic;    /* used for convergence test */
        oib = bitemp->oib;
        delvbe = vbe - ovbe;
        delvbc = vbc - ovbc;

        vbe = pnjlim(vbe,ovbe,vt,is,vcritbe);
        vbc = pnjlim(vbc,ovbc,vt,is,vcritbc);

        if (vbe <= -5.0*vt) {
                gmf = 1.0e-15;
                icc = gmf*vbe;
                ib1 = -ise;
                g1 = ib1/vbe;
        }
        else {
                icc = is*(exp(vbe/vt) - 1);
                gmf = (icc+is)/vt;
                ib1 = ise*(exp(vbe/(ne*vt)) - 1);
```

```
                g1 = (ib1+ise)/(ne*vt);
        }
        if (vbc <= -5.0*vt) {
                gmr = 1.0e-15;
                ice = gmr*vbc;
                ib2 = -isc;
                g2 = ib2/vbc;
        }
        else {
                ice = is*(exp(vbc/vt) - 1);
                gmr = (ice+is)/vt;
                ib2 = isc*(exp(vbc/(nc*vt)) - 1);
                g2 = (ib2+isc)/(nc*vt);
        }

        if(ovaf!=0 || ovar!=0)
                q1 = 1/(1-vbc*ovaf-vbe*ovar);
        else
                q1 = 1.0;
        if(oikf!=0 || oikr!=0) {
                q2 = icc*oikf + ice*oikr;
                /* Spice code for qb implementation */
                qb = q1*(1 + sqrt(1+4*q2))/2;
                dqbdvbe = q1*(qb*ovar + gmf*oikf/sqrt(1+4*q2));
                dqbdvbc = q1*(qb*ovaf + gmr*oikr/sqrt(1+4*q2));
                /* This is the exact formula from GP
                sqarg = sqrt((q1*q1/4)+q2);
                qb = q1/2+sqarg;
                dqbdvbe = q1*q1*ovar/2;
                dqbdvbe += (q1*q1*q1*ovar/2 + gmf*oikf)/(2*sqarg);
                dqbdvbc = q1*q1*ovaf/2;
                dqbdvbe += (q1*q1*q1*ovaf/2 + gmr*oikr)/(2*sqarg);
                */

        }
        else {
                qb = q1;
                dqbdvbe = q1*q1*ovar;
                dqbdvbc = q1*q1*ovaf;
        }

        gc = 1/rmax; /* rc does not modulate in GP */

        ic = (icc-ice)/qb - ib2 - ice/br;
        ib = icc/bf + ice/br + ib1 + ib2;
        /* rb modulates if rbm specified */
        gb *= qb;
        gpi = gmf/bf + g1;
        gmu = gmr/br + g2;
        go = (gmr + (icc-ice)*dqbdvbc/qb)/qb;
        gm = (gmf - (icc-ice)*dqbdvbe/qb)/qb - go;
        icfn = icc - gmf*vbe;
        icrn = ice - gmr*vbc;
        ib1n = ib1 - g1*vbe;
        ib2n = ib2 - g2*vbc;

        /* These are set to 0 here for convergence later */

        gcbc = 0.0;
        bitemp->ibici = 0.0;
        gcbe = 0.0;
        bitemp->ibiei = 0.0;

        if (atype == 1) {
```

```
gcbc = 0.0;
capbc = 0.0;
bitemp->ibici = 0.0;    /* BC cap current */
bitemp->qbici = 0.0;    /* BC cap charge  */
gcbxc = 0.0;
capbxc = 0.0;
bitemp->ibxci = 0.0;    /* Ext BC cap current */
bitemp->qbxci = 0.0;    /* Ext BC cap charge  */
gcbe = 0.0;
gcbebc = 0.0;
capbe = 0.0;
bitemp->ibiei = 0.0;
bitemp->qbiei = 0.0;
gcsc = 0.0;
capsc = 0.0;
bitemp->iscn = 0.0;
bitemp->qscn = 0.0;

/* calculate the caps and charge   */

xcjc = btemp->bmptr->xcjc;
cjc = btemp->bmptr->cjc*btemp->ae*xcjc;
cjbxc = btemp->bmptr->cjc*btemp->ae*(1.0 - xcjc);
vjc = btemp->bmptr->vjc;
mjc = btemp->bmptr->mjc;
cje = btemp->bmptr->cje*btemp->ae;
vje = btemp->bmptr->vje;
mje = btemp->bmptr->mje;
cjs = btemp->bmptr->cjs*btemp->ae;
vjs = btemp->bmptr->vjs;
mjs = btemp->bmptr->mjs;
fc = btemp->bmptr->fc;
tr = btemp->bmptr->tr;
tf = btemp->bmptr->tf;


if(cjc != 0)
        deplcap(&capbc,&bitemp->qbici,vbc,cjc,vjc,mjc,fc);
        deplcap(&capbxc,&bitemp->qbxci,vbxc,cjbxc,vjc,mjc,fc);
bitemp->qbici += tr*ice; /* + deplcharge */
capbc += tr*gmr; /* + cjc*sarg;  BC cap value */
if(cje != 0)
        deplcap(&capbe,&bitemp->qbiei,vbe,cje,vje,mje,fc);
bitemp->qbiei += tf*icc/qb;
capbe += tf*(gmf-icc*dqbdvbe/qb)/qb;
/* gcbebc is transcapacitance, dQbe/dVbc   */
gcbebc = -tf*icc*dqbdvbc/(qb*qb);
if(cjs != 0)
        deplcap(&capsc,&bitemp->qscn,vsc,cjs,vjs,mjs,0.0);
if(tritct==0 && orinc==0) {
        bitemp->oqbici = bitemp->qbici;
        bitemp->oqbxci = bitemp->qbxci;
        bitemp->oqbiei = bitemp->qbiei;
        bitemp->oqscn = bitemp->qscn;
}

intb8(&gcbc,&bitemp->ibici,bitemp->oqbici,
          bitemp->qbici,bitemp->oibici,capbc);
irhsbc = gcbc*vbc - bitemp->ibici;
intb8(&gcbxc,&bitemp->ibxci,bitemp->oqbxci,
          bitemp->qbxci,bitemp->oibxci,capbxc);
irhsbxc = gcbxc*vbxc - bitemp->ibxci;
intb8(&gcbe,&bitemp->ibiei,bitemp->oqbiei,
          bitemp->qbiei,bitemp->oibiei,capbe);
```

```
        if (order == 1)    /* backward Euler */
                gcbebc /= tstep;
        else   /* trapezoidal    */
                gcbebc *=2.0/tstep;
        irhsbe = gcbe*vbe + gcbebc*vbc - bitemp->ibiei;
        intb8(&gcsc,&bitemp->iscn,bitemp->oqscn,
                    bitemp->qscn,bitemp->oiscn,capsc);
        irhssc = gcsc*vsc - bitemp->iscn;

}

/* Check for convergence     */
 * Note that ic and ib are just dc currents so
 * iccon and ibcon have the cap current terms
 * added in also  */


iccon = ic - bitemp->ibici;
ibcon = ib + bitemp->ibici + bitemp->ibiei;
if(abs(iccon-oic) >= reltol*max(abs(iccon),abs(oic)) + abstol)
        ++nocon;
else {
if(abs(ibcon-oib) >= reltol*max(abs(ibcon),abs(oib)) + abstol)
        ++nocon;
}
bitemp->oic=iccon+(gm+go)*delvbe-(go+gmu+gcbc)*delvbc;
bitemp->oib=ibcon+(gpi+gcbe)*delvbe+(gmu+gcbc)*delvbc;


if (bitemp->bpt33) bitemp->bpt33->value +=go+gmu+gmin+gc;
if (bitemp->bpt35) bitemp->bpt35->value +=gm-gmu;
if (bitemp->bpt37) bitemp->bpt37->value -=gm+go;
if (bitemp->bpt53) bitemp->bpt53->value -=gmu;
if (bitemp->bpt55) bitemp->bpt55->value +=gmu+gpi+gmin+gb;
if (bitemp->bpt57) bitemp->bpt57->value -=gpi;
if (bitemp->bpt73) bitemp->bpt73->value -=go;
if (bitemp->bpt75) bitemp->bpt75->value -=gm+gpi;
if (bitemp->bpt77) bitemp->bpt77->value +=go+gpi+gm+gmin+ge;
if (bitemp->bpt11) bitemp->bpt11->value +=gbl;
if (bitemp->bpt12) bitemp->bpt12->value -=gbl;
if (bitemp->bpt21) bitemp->bpt21->value -=gbl;
if (bitemp->bpt22) bitemp->bpt22->value +=gbl+gc;
if (bitemp->bpt23) bitemp->bpt23->value -=gc;
if (bitemp->bpt32) bitemp->bpt32->value -=gc;
if (bitemp->bpt44) bitemp->bpt44->value +=gb;
if (bitemp->bpt45) bitemp->bpt45->value -=gb;
if (bitemp->bpt54) bitemp->bpt54->value -=gb;
if (bitemp->bpt66) bitemp->bpt66->value +=ge;
if (bitemp->bpt67) bitemp->bpt67->value -=ge;
if (bitemp->bpt76) bitemp->bpt76->value -=ge;
if (bitemp->bpt28) bitemp->bpt28->value -=0.0;
if (bitemp->bpt82) bitemp->bpt82->value -=0.0;
if (bitemp->bpt88) bitemp->bpt88->value +=gmin;

if (bitemp->brhs3)
        bitemp->brhs3->rhvalue +=type*((gm+go)*vbe-(gmu+go)*vbc-ic);
if (bitemp->brhs5)
        bitemp->brhs5->rhvalue +=type*(gpi*vbe+gmu*vbc-ib);
if (bitemp->brhs7)
        bitemp->brhs7->rhvalue +=type*(go*vbc-(gm+go+gpi)*vbe+ic+ib);
if (bitemp->brhs2) bitemp->brhs2->rhvalue +=0.0;
if (bitemp->brhs8) bitemp->brhs8->rhvalue +=0.0;


if (atype == 1)  {
```

```
					if (bitemp->bpt33) bitemp->bpt33->value +=gcbc;
					if (bitemp->bpt35) bitemp->bpt35->value -=gcbc;
					if (bitemp->bpt53) bitemp->bpt53->value -=gcbc + gcbebc;
					if (bitemp->bpt55) bitemp->bpt55->value +=
								gcbc + gcbe + gcbebc;
					if (bitemp->bpt57) bitemp->bpt57->value -=gcbe;
					if (bitemp->bpt75) bitemp->bpt75->value -=gcbe + gcbebc;
					if (bitemp->bpt77) bitemp->bpt77->value +=gcbe;
					if (bitemp->bpt22) bitemp->bpt22->value +=gcsc;
					if (bitemp->bpt28) bitemp->bpt28->value -=gcsc;
					if (bitemp->bpt82) bitemp->bpt82->value -=gcsc;
					if (bitemp->bpt88) bitemp->bpt88->value +=gcsc;
					if (bitemp->bpt73) bitemp->bpt73->value +=gcbebc;

					if (bitemp->brhs3)
						bitemp->brhs3->rhvalue -= type*(irhsbc+irhsbxc);
					if (bitemp->brhs4)
						bitemp->brhs4->rhvalue += type*irhsbxc;
					if (bitemp->brhs5)
						bitemp->brhs5->rhvalue += type*(irhsbc+irhsbe);
					if (bitemp->brhs7)
						bitemp->brhs7->rhvalue -= type*irhsbe;
					if (bitemp->brhs2)
						bitemp->brhs2->rhvalue -= type*irhssc;
					if (bitemp->brhs8)
						bitemp->brhs8->rhvalue += type*irhssc;

				}

				bitemp->ovbiei = vbe;
				bitemp->ovbici = vbc;

				bitemp = bitemp->nextbim;

			}
		}
}
```

intb8

```
/* Trapezoidal integrating routine for bjt's */

intb8(gcap,icap,oldq,newq,oldicap,cap)
float *gcap, *icap, oldq, newq, oldicap, cap;

{
	extern int order;
	extern float tstep;

	if (order == 1) {	/*backward Euler */
		*gcap = cap/tstep;
		*icap = (newq - oldq)/tstep;
	}
	else {	/* trapezoidal */
		*gcap = 2.0*cap/tstep;
		*icap = -oldicap + 2.0*(newq - oldq)/tstep;
	}
}
```

deplcap

```
/* Routine for calculating depletion cap and charge */

deplcap(cap,q,v,cj,vj,mj,fc)
float *cap,*q,v,cj,vj,mj,fc;

{
	float arg,sarg,f1,f2,f3;
```

```
        if (v  <= fc*vj) {
                arg = 1.0 - v/vj;
                sarg = pow(arg,-mj);
                *q = cj*vj*(1.0-arg*sarg)/(1.0-mj);
                *cap = cj*sarg;
        }
        else {  /* v > fc*vj  */
                f1 = vj*(1.0-pow(1.0-fc,1.0-mj))/(1.0-mj);
                f2 = pow(1.0-fc,mj+1.0);
                f3 = 1.0 - fc*(mj+1.0);
                *cap = cj*(f3+mj*v/vj)/f2;
                *q=cj*f1+cj*(f3*(v-fc*vj)+mj*(v*v-fc*fc*vj*vj)/(2.0*vj))/f2;
        }
}
```

APPENDIX G: LISTING OF THE TURGEON-MATHEWS MODEL FUNCTION

```
/*
 *  This file, tm.c, contains the Turgeon-Mathews
 *  bipolar model evaluation.
 */
#include "types.h"
#include "extern.h"
#include "defs.h"
#define max(a,b) ((a) > (b) ? (a) : (b))
#define min(a,b) ((a) < (b) ? (a) : (b))
#define abs(a)   ((a) < 0.0 ? -(a) : (a))
#define sign(a,b) ((b) < 0.0 ? -abs(a) : abs(a))

extern double     abstol, reltol, vntol, trtol;
extern int                orinc;
```

tm

```
tm(atype)
int atype;

{
        float Is, I1, I2, I3, I4, I5, I6, ne, nc, Ikf, Ikr, vaf, var;
        float oIkf, oIkr, ovaf, ovar, vt, vcritbe, vcritbc;
        float vbe, vbc, vbxc, vcnci, vsc, ovbe, ovbc, type;
        float ib1, ib2, ib3, ib4, icc, icf, icr, qb, pond, ibcc, xowc;
        float cjeo, phie, mje, cjco, phic, mjc, tfo, tro, heo, hco, hdc;
        float Rm, Ge, Gb, Gbl, Gc, tlr, ar, dare, darc, icco, n, npc;
        float cBEterm, cBCterm, qBEterm, qBCterm;
        float ebe, ebc, BEfactor, BCfactor, ge, gc, he, hc, fe, fc;
        float gmf, gmr, gpi, gmu, ic, ib, icrhs, ibrhs;
        float dgedvbe, dgcdvbc, dhedvbe, dhcdvbc, dfedvbe, dfedvbc;
        float dfcdvbe, dfcdvbc, dqbdvbe, dqbdvbc, diccdvbe, diccdvbc;
        float dib1dvbe, dib2dvbe, dib3dvbc, dib4dvbc, dponddvbc;
        float dibccdvbe, dibccdvbc, dGcdvbe, dGcdvbc, gGcbc, gGcbe, iGcrhs;
        float cjso, phis, mjs, cCSterm, Csub, gCsub, iQsubrhs:
        float dQbedvbe, dQbedvbc, dQbcdvbe, dQbcdvbc, dQcdvbc, dQcdvbe;
        float gQbevbe, gQbevbc, gQbcvbc, gQbcvbe, gQcvbc, gQcvbe;
        float iQberhs, iQbcrhs, iQcrhs, Qco;
        float delvbe, delvbc, iccon, ibcon, oib, oic;
        float dxowcdicc, oicc, doicc, iccm, icrwd, icrwd1;
        float oiccrd, doiccrd, art, ccrd1;
        float Vp, oVp, xjeo, xjco, Wbo;
        float alpha, ibd, ogmf, ogmr, ogmu, ogpi, ogQbcvbc, ogQbcvbe;
        float ogQbevbe, ogQbevbc, ogQcvbe, ogQcvbc;
        float pnjlim(), gmin;
        double exp(), log(), sqrt(), pow();

        struct bjt *btemp;
        struct bjtimfo *bitemp;

        extern float vtherm, tstep, ni, nit;
        extern int nocon, tritct;
        extern struct bjt *bjt;

        gmin = fvalue("gmin");

        for (btemp = bjt; btemp; btemp = btemp->nextbjt) {
                bitemp = btemp->bim;

                Is = btemp->bmptr->Is*btemp->ae;
                I1 = btemp->bmptr->I1*btemp->ae;
                I2 = btemp->bmptr->I2*btemp->ae;
                I3 = btemp->bmptr->I3*btemp->ae;
                I4 = btemp->bmptr->I4*btemp->ae;
                I5 = btemp->bmptr->I5*btemp->ae;
                I6 = btemp->bmptr->I6*btemp->ae;
                ne = btemp->bmptr->ne;
```

```
nc = btemp->bmptr->nc;
vaf = btemp->bmptr->vaf;
var = btemp->bmptr->var;
Ikf = btemp->bmptr->Ikf*btemp->ae;
Ikr = btemp->bmptr->Ikr*btemp->ae;
cjeo = btemp->bmptr->cjeo*btemp->ae;
phie = btemp->bmptr->phie;
mje = btemp->bmptr->mje;
cjco = btemp->bmptr->cjco*btemp->ae;
phic = btemp->bmptr->phic;
mjc = btemp->bmptr->mjc;
tfo = btemp->bmptr->tfo;
tro = btemp->bmptr->tro;
heo = btemp->bmptr->heo;
hco = btemp->bmptr->hco;
hdc = btemp->bmptr->hdc;
icco = btemp->bmptr->icco;
n = btemp->bmptr->n;
npc = btemp->bmptr->npc;
iccm = btemp->bmptr->iccm;
ibd = btemp->bmptr->ibd;          /* Have yet to add the parasitic diode */
Rm = btemp->bmptr->Rm/btemp->ae; /* Rc will be affected by crwd */
Ge = btemp->ae/btemp->bmptr->Re;
Gb = btemp->ae/btemp->bmptr->Rb;
Gbl = btemp->ae/btemp->bmptr->Rbl;
/*
 * If Vp = 0, then it is calculated
 * below using the punchthrough condition of fe=0
 * and Qbo+Qje+Qjc=0
 */
tlr = 2/( 3 - I6/I5);
if ( vaf==0)
        ovaf = 0.0;
else
        ovaf = 1/vaf;
if ( var==0)
        ovar = 0.0;
else
        ovar = 1/var;
if ( Ikf==0)
        oIkf = 0.0;
else
        oIkf = 1/Ikf;
if ( Ikr==0)
        oIkr = 0.0;
else
        oIkr = 1/Ikr;
Vp = 1+(1-mjc)*vaf/phic+phie*vaf*ovar*(1-mjc)/((1-mje)*phic);
Vp = vaf*( pow(Vp, mjc/(1-mjc)) - 1 - var/vaf);
oVp = 1/Vp;
vt = vtherm;
type = 1.0;  /* default to a npn device  */
if( !btemp->bmptr->btype) type = -1.0;  /* pnp device */

while(bitemp) {
        vbe = 0.0;
        vbc = 0.0;
        vbxc = 0.0;
        vsc = 0.0;
        vcnci = 0.0;
        dqbdvbe = 0.0;
        dqbdvbc = 0.0;
```

```
/*
 *  Calculate the junction voltages of the device
 */
if (bitemp->nbivalue) {
        vbe = type*bitemp->nbivalue->ovalue;
        vbc = vbe;
}
if (bitemp->neivalue) {
        vbe -= type*bitemp->neivalue->ovalue;
}
if (bitemp->nbxvalue) {
        vbxc = type*bitemp->nbxvalue->ovalue;
}
if (bitemp->ncivalue) {
        vbc -= type*bitemp->ncivalue->ovalue;
        vcnci -= type*bitemp->ncivalue->ovalue;
        vbxc -= type*bitemp->ncivalue->ovalue;
}
if (bitemp->ncnvalue) {
        vsc -= type*bitemp->ncnvalue->ovalue;
        vcnci += type*bitemp->ncnvalue->ovalue;
}
if (bitemp->nsvalue) {
        vsc += type*bitemp->nsvalue->ovalue;
}

/*
 * Limit the voltage across the junctions
 */
ovbe = bitemp->ovbiei;
ovbc = bitemp->ovbici;
oic = bitemp->oic;
oib = bitemp->oib;
delvbe = vbe - ovbe;
delvbc = vbc - ovbc;
tmjlim(&vbe, ovbe, vt, phie);
tmjlim(&vbc, ovbc, vt, phic);

/*
 * Define terms that are used in many equations
 * cBEterm is for the BE depletion cap eqn
 * cBCterm is for the BC depletion cap eqn
 * qBEterm is for the qb BE depl region charge
 * qBCterm is for the qb BC depl region charge
 */
ebe = exp(vbe/vt);
ebc = exp(vbc/vt);
BEfactor = ebe*exp( -phie/vt);   /* exp((vbe-phie)/vt) */
BCfactor = ebc*exp( -phic/vt);   /* exp((vbc-phic)/vt) */
cBEterm = pow( 1 - vbe/phie, -mje);
cBCterm = pow( 1 - vbc/phic, -mjc);
qBEterm = cBEterm*( 1 - vbe/phie); /* pow(1-vbe/phie,1-mje) */
qBCterm = cBCterm*( 1 - vbc/phic); /* pow(1-vbc/phic,1-mjc) */

/*
 *  Calculate the g, h, and f terms.
 *  g is the high injection factor
 *  h is for high injection in the base
 *  f if for modulated base charge due to Early Effect
 *  The terms beginning with d correspond to derivative
 *  terms (i.e. dgedvbe means the partial of ge with
 *  respect to vbe).
 */
ge = 1/( 1 - BEfactor);
gc = 1/( 1 - BCfactor);
```

```
he = 1 + heo*ebe*ge;
hc = 1 + hco*ebc*gc;
fe = 1.0 + oVp*(var*( 1 - 1/cBEterm) + vaf*( 1 - 1/cBCterm));
fc = fe;
fe *= cBEterm;
fc *= cBCterm;
dgedvbe = ge*ge*BEfactor/vt;
dgcdvbc = gc*gc*BCfactor/vt;
dhedvbe = heo*ebe*( ge/vt + dgedvbe);
dhcdvbc = hco*ebc*( gc/vt + dgcdvbc);
dfedvbe = (fe + var*oVp)*mje/(phie - vbe);
dfedvbc = vaf*oVp*mjc*cBEterm/( phic*qBCterm);
dfcdvbc = (fc + vaf*oVp)*mjc/(phic - vbc);
dfcdvbe = var*oVp*mje*cBCterm/( phie*qBEterm);
/*
* Calculate the current terms.
*  ib1 is the Is/Bf base current
*  ib2 is the BE recomb/gen current
*  ib3 is the Is/Br base current
*  ib4 is the BC recomb/gen current
*  ibcc is the collector recomb current
*  icf is the forward transport current
*  icr is the reverse transport current
*  icc is the transport current including qb modulation
*  qb is the normalized base charge due to 5 terms:
*               built-in charge, BE diff charge, BE depl charge,
*               BC diff charge, BC depl charge
*/
ib1 = I1*(ebe - 1)*ge;
ib2 = I2*(exp(vbe/(ne*vt)) - 1)*ge;
ib3 = I3*(ebc - 1)*gc;
ib4 = I4*(exp(vbc/(nc*vt)) - 1)*gc;
icf = Is*ebe*ge*he;
icr = Is*ebc*gc*hc;
qb = 1.0;
if ( ovar!=0) {
        qb += phie*ovar*( 1 - qBEterm)/( 1 - mje);
        dqbdvbe += ovar*cBEterm; /* pow(1-vbe/vt,-mje)/var */
}
if ( ovaf!=0) {
        qb += phic*ovaf*( 1 - qBCterm)/( 1 - mjc);
        dqbdvbc += ovaf*cBCterm; /* pow(1-vbc/vt,-mjc)/vaf */
}
if ( oIkf!=0) {
        qb += Is*oIkf*( ebe -1)*ge*fe;
        dqbdvbe += Is*oIkf*ebe*ge*fe/vt;
        dqbdvbe += Is*oIkf*( ebe - 1)*( fe*dgedvbe + ge*dfedvbe);
        dqbdvbc += Is*oIkf*( ebe - 1)*ge*dfedvbc;
}
if ( oIkr!=0) {
        qb += Is*oIkr*( ebc - 1)*gc*fc;
        dqbdvbc += Is*oIkr*ebc*gc*fc/vt;
        dqbdvbc += Is*oIkr*( ebc - 1)*( fc*dgcdvbc + gc*dfcdvbc);
        dqbdvbe += Is*oIkr*( ebc - 1)*gc*dfcdvbe;
}
icc = ( icf - icr)/qb;
if ( abs(icc) <= 1.0e-18) icc = 1.e-18;
diccdvbe = (icf/vt + icf*dgedvbe/ge + icf*dhedvbe/he)/qb;
diccdvbe -= icc*dqbdvbe/qb;
diccdvbc = (-icr/vt - icr*dgcdvbc/gc - icr*dhcdvbc/hc)/qb;
diccdvbc -= icc*dqbdvbc/qb;
dib1dvbe = ib1*dgedvbe/ge + (ib1 + ge*I1)/vt;
dib2dvbe = ib2*dgedvbe/ge + (ib2 + ge*I2)/( ne*vt);
dib3dvbc = ib3*dgcdvbc/gc + (ib3 + gc*I3)/vt;
dib4dvbc = ib4*dgcdvbc/gc + (ib4 + gc*I4)/( nc*vt);
```

```
/*
 *  Calculate the current crowding terms
 *  ar is Ae' /Ae ... the area reduction
 *  dare is d(ar)/d\be
 *  darc is d(ar)/d\bc
 */
if ( npc == 0 || npc == 1.0) {
        /* add curfit here to not let 1/icc get too large
         * The curfit function can cause accuracy problems
         * for low currents...I prefer the implementation
         * without the curfit function
        curfit( &oicc, &doicc, icc, iccm);
        ar = 1/( 1 + pow( (1/(oicc*icco)), n));
        dare = -ar*ar*n*pow((1/(oicc*icco)),n)*diccdvbe*oicc;
        darc = -ar*ar*n*pow((1/(oicc*icco)),n)*diccdvbc*oicc;
        */
        /* Without curfit for icc in the ar eqn */
        icrwd = icc/icco;
        if ( icrwd < 1e-3) {
                ar = 1.0;
                dare = 0;
                darc = 0;
        }
        else {
                icrwd1 = pow(icrwd, n-1);
                ar = 1/( 1 + icrwd1*icrwd);
                dare = -ar*ar*n*icrwd1*diccdvbe/icco;
                darc = -ar*ar*n*icrwd1*diccdvbc/icco;
        }
}
else {
        /* Note that by using the curfit function that the
         * returned value for 1/icc can be somewhat different
         * from the actual value.  But the curfit function
         * helps the ar reduction fit because the ar equation
         * usedis by no means exact.
         */
        /* This is Turgeon's code for curve fitting low icc */
        /*
        ccrd1 = 5.*icco/3.;
        curfit( &oiccrd, &doiccrd, icc, ccrd1);
        art = pow((icco*oiccrd), n);
        ar = ( 1. - npc)*art + npc;
        dare = ( 1. - npc)*n*art*doiccrd/oiccrd;
        darc = dare;
        dare *= diccdvbe;
        darc *= diccdvbc;
        */
        /* My version of Turgeon's  */
        icrwd = icc/icco;
        if ( icrwd < 1e-3) {
                ar = 1.0;
                dare = 0;
                darc = 0;
        }
        else {
                icrwd1 = pow(icrwd, n-1);
                ar = 1/( 1 + icrwd1*icrwd);
                dare = ar*ar;
                darc = dare;
                ar = (1 - npc)*ar + npc;
                dare *= -(1 - npc)*n*icrwd1*diccdvbe/icco;
                darc *= -(1 - npc)*n*icrwd1*diccdvbc/icco;
        }
}
```

```
/*
 *  Calculate ibcc and its derivatives
 *  Note that pond ( po/Ndc) is used in the ibcc
 *  expression.
 *  pond is the ratio of the minority carriers at the C side
 *  of the BC jcn (po) to the collector epy doping (Ndc)
 *  First use a curve-fit routine to smooth out 1/icc and
 *  its derivative so that it won't give us problems
 */
curfit( &oicc, &doicc, icc, iccm);
pond = hdc*( ebc - 1)*gc;
dponddvbc = pond*dgcdvbc/gc + (pond + gc*hdc)/vt;
ibcc = (I5 - I6/tlr)*log( tlr*pond + 1) + I6*pond + I5*pond*pond;
ibcc *= ar*Is*oicc;
dibccdvbe = ibcc*doicc*diccdvbe/oicc + ibcc*dare/ar;
dibccdvbc = (I5*tlr - I6)/( tlr*pond + 1) + I6 + 2*I5*pond;
dibccdvbc *= ar*(Is/icc)*dponddvbc;
dibccdvbc += ibcc*doicc*diccdvbc/oicc + ibcc*darc/ar;
/*
 *  Calculate the modulated collector resistance.
 *  The expression xowc is a normalized position
 *  that determines how much of the collector
 *  region is modulated.
 *  xowc is a function of the BC bias and
 *  the transport current term (icc).
 *  The terms beginning with 'd' are dervatives of
 *  the collector admittance with respect to Vbe
 *  and Vbc: dGcdvbe and dGcdvbc, respectively.
 *  The terms beginning with 'g' are "transadmittance"
 *  terms that go in the admittance matrix.
 *  iGcrhs is the contribution due to Rc that is added
 *  to the rhs of the nodal equations.
 */
xowc = vt*( 2*pond - 1)*oicc/Rm;
dxowcdicc = vt*( 2*pond - 1)*doicc/Rm;
if ( xowc > 8) xowc = 8.0;
Gc = ar*(1 + exp( -2*( 1 - 2*xowc)))/Rm;
dGcdvbe = 4*( Gc - ar/Rm)*dxowcdicc*diccdvbe;
dGcdvbe += Gc*dare/ar;
dGcdvbc = 4*( Gc - ar/Rm);
dGcdvbc *= 2*vt*dponddvbc*oicc/Rm + dxowcdicc*diccdvbc;
dGcdvbc += Gc*darc/ar;
gGcbe = -vcnci*dGcdvbe;
gGcbc = -vcnci*dGcdvbc;
iGcrhs = gGcbe*vbe + gGcbc*vbc;
/*
 *  Modulate the internal base resistance
 *  rb = rb/qb
 *  Should add in the derivative terms for companion
 *  model and for convergence (it is not done in
 *  Spice either)
 */
Gb *= qb;
/*
 *  The terms due to the internal diodes and VCCS
 *  that go into the admittance matrix and rhs
 *  of the nodal equations are calculated.
 *  The terms beginning with 'g' are
 *  transconductances:
 *  gmf = dic/dVbe
 *  gmr = dic/dVbc
 *  gpi = dib/dVbe
 *  gmu = dib/dVbc
 *  The collector and base currents are calculated as:
 *  ic = icc - ib3 - ib4 - ibcc
```

```
*  ib = ib1 + ib2 + ib3 + ib4 + ibcc
*  ( ie = -ic -ib),  ie = emitter current
*  The contributions the rhs of the nodal equations are:
*  icrhs for the internal collector node
*  ibrhs for the internal base node
*  ierhs (for the internal emitter node) = -icrhs - ierhs
*/
gmf = diccdvbe - dibccdvbe;
gmr = diccdvbc - dib3dvbc - dib4dvbc - dibccdvbc;
gpi = dib1dvbe + dib2dvbe + dibccdvbe;
gmu = dib3dvbc + dib4dvbc + dibccdvbc;
ic = icc - ib3 - ib4 - ibcc;
icrhs = gmf*vbe + gmr*vbc -ic;
ib = ib1 + ib2 + ib3 + ib4 + ibcc;
ibrhs = gpi*vbe + gmu*vbc - ib;
/*
*  These values are set to 0 here for non-transient
*  analysis so that they will not affect the convergence
*/
bitemp->iQbc = 0.0;
bitemp->iQc = 0.0;
bitemp->iQbe = 0.0;
gQbevbe = 0.0;
gQbevbc = 0.0;
gQbcvbc = 0.0;
gQbcvbe = 0.0;
gQcvbe = 0.0;
gQcvbc = 0.0;
/*
*  Calculate the needed terms for the transient analysis
*  These terms are due to the charge stored at the
*  BE, BC, CS junctions.
*  Qbe is the sum of the junction BE depletion charge, Qje,
*  and the BE diffusion charge, Qde.
*  Qbc is the sum of the junction BC depletion charge, Qjc,
*  and the BC diffusion charge, Qdc.
*  Qc is the epitaxial collector free electron-hole diffusion
*  collector charge.
*/
if (atype == 1) {
        Qco = btemp->bmptr->Qco;
        cjso = btemp->bmptr->cjso*btemp->ae;
        phis = btemp->bmptr->phis;
        mjs = btemp->bmptr->mjs;
        cCSterm = pow(1 - vsc/phis, -mjs);
        bitemp->Qbe = phie*cjeo*( 1 - qBEterm)/( 1 - mje);
        bitemp->Qbe += Is*tfo*( ebe - 1)*ge*fe;
        bitemp->Qbc = phic*cjco*( 1 - qBCterm)/( 1 - mjc);
        bitemp->Qbc += Is*tro*( ebc - 1)*gc*fc;
        bitemp->Qc = Is*Qco*( pond + pond*pond)/icc;
        bitemp->Qsub = phis*cjso*(1-cCSterm*(1-vsc/phis))/(1-mjs);
        /*
        *  Calculate the derivatives of Qbe w.r.t. Vbe and Vbc
        */
        dQbedvbe = cjeo*cBEterm + Is*tfo*ebe*ge*fe/vt;
        dQbedvbe += Is*tfo*( ebe - 1)*( fe*dgedvbe + ge*dfedvbe);
        dQbedvbc = Is*tfo*( ebe - 1)*ge*dfedvbc;
        /*
        *  Calculate the derivatives of Qbc w.r.t. Vbe and Vbc
        */
        dQbcdvbc = cjco*cBCterm + Is*tro*ebc*gc*fc/vt;
        dQbcdvbc += Is*tro*( ebc - 1)*( fc*dgcdvbc + gc*dfcdvbc);
        dQbcdvbe = Is*tro*( ebc - 1)*gc*dfcdvbe;
```

```
        /*
         *  Calculate the derivatives of Qc w.r.t Vbe and Vbc
         */
        dQcdvbc = Is*Qco*( 1 + 2*pond)*dponddvbc/icc;
        dQcdvbc -= bitemp->Qc*diccdvbc/icc;
        dQcdvbe = -bitemp->Qc*diccdvbe/icc;
        /*
         *  Calculate the derivative of Qsub w.r.t Vsc
         *  This is the depletion cap of the Collector-
         *  Substrate junction, Csub.
         */
        Csub = cjso*cCSterm;
        /*
         *  If at the very first iteration at a time point
         *  then need to have a value for the old charge
         *  to be used in the integration method that relates
         *  charge to current.
         */
        if ( tritct==0 && orinc==0) {
                bitemp->oQbe = bitemp->Qbe;
                bitemp->oQbc = bitemp->Qbc;
                bitemp->oQc = bitemp->Qc;
                bitemp->oQsub = bitemp->Qsub;
        }
        /*
         *  Calculate the terms to be added to the nodal equations
         *  Those beginning with 'g' are added to the admittance
         *  matrix and those beginning with 'i' and ending
         *  with 'rhs' are added to the rhs of the nodal
         *  equations.
         */
        CapAdmittance( &gQbevbe, dQbedvbe);
        CapAdmittance( &gQbevbc, dQbedvbc);
        CapCurrent( &bitemp->iQbe, bitemp->Qbe,
                        bitemp->oQbe, bitemp->oiQbe);
        iQberhs = gQbevbe*vbe + gQbevbc*vbc - bitemp->iQbe;
        CapAdmittance( &gQbcvbc, dQbcdvbc);
        CapAdmittance( &gQbcvbe, dQbcdvbe);
        CapCurrent( &bitemp->iQbc, bitemp->Qbc,
                        bitemp->oQbc, bitemp->oiQbc);
        iQbcrhs = gQbcvbc*vbc + gQbcvbe*vbe - bitemp->iQbc;
        CapAdmittance( &gQcvbc, dQcdvbc);
        CapAdmittance( &gQcvbe, dQcdvbe);
        CapCurrent( &bitemp->iQc, bitemp->Qc,
                        bitemp->oQc, bitemp->oiQc);
        iQcrhs = gQcvbc*vbc + gQcvbe*vbe - bitemp->iQc;
        CapAdmittance( &gCsub, Csub);
        CapCurrent( &bitemp->iQsub, bitemp->Qsub,
                        bitemp->oQsub, bitemp->oiQsub);
        iQsubrhs = gCsub*vsc - bitemp->iQsub;
}
/*
 *  Check for convergence
 */
iccon = ic - bitemp->iQbc - bitemp->iQc;
ibcon = ib + bitemp->iQbe + bitemp->iQbc + bitemp->iQc;
if( abs(iccon-oic) >= reltol*max(abs(iccon),abs(oic)) + abstol)
        ++nocon;
else if( abs(ibcon-oib) >= reltol*max(abs(ibcon),abs(oib)) + abstol)
        ++nocon;
bitemp->oic = iccon + (gmf - gQbcvbe - gQcvbe)*delvbe;
bitemp->oic += (gmr - gQbcvbc - gQcvbc)*delvbc;
bitemp->oib = ibcon + (gpi + gQbevbe + gQbcvbe + gQcvbe)*delvbe;
bitemp->oib += (gmu + gQbcvbc + gQbevbc + gQcvbc)*delvbc;
```

```
/*
 *  Enter the terms into the admittance matrix and
 *  the rhs of the nodal equations.
 *  Note that if the node is grounded, then nothing
 *  is added.
 */
if (bitemp->bpt11) bitemp->bpt11->value += Gbl;
if (bitemp->bpt12) bitemp->bpt12->value -= Gbl;
if (bitemp->bpt21) bitemp->bpt21->value -= Gbl;
if (bitemp->bpt22) bitemp->bpt22->value += Gbl + Gc;
if (bitemp->bpt23) bitemp->bpt23->value += gGcbc - Gc;
if (bitemp->bpt25) bitemp->bpt25->value -= gGcbe + gGcbc;
if (bitemp->bpt27) bitemp->bpt27->value += gGcbe;
if (bitemp->bpt32) bitemp->bpt32->value -= Gc;
if (bitemp->bpt33) bitemp->bpt33->value -= gmr + gGcbc -Gc;
if (bitemp->bpt35) bitemp->bpt35->value += gmf +gmr +gGcbe +gGcbc;
if (bitemp->bpt37) bitemp->bpt37->value -= gmf + gGcbe;
if (bitemp->bpt44) bitemp->bpt44->value += Gb;
if (bitemp->bpt45) bitemp->bpt45->value -= Gb;
if (bitemp->bpt53) bitemp->bpt53->value -= gmu;
if (bitemp->bpt54) bitemp->bpt54->value -= Gb;
if (bitemp->bpt55) bitemp->bpt55->value += gpi + gmu + Gb;
if (bitemp->bpt57) bitemp->bpt57->value -= gpi;
if (bitemp->bpt66) bitemp->bpt66->value += Ge;
if (bitemp->bpt67) bitemp->bpt67->value -= Ge;
if (bitemp->bpt73) bitemp->bpt73->value += gmr + gmu;
if (bitemp->bpt75) bitemp->bpt75->value -= gmf + gpi + gmr + gmu;
if (bitemp->bpt76) bitemp->bpt76->value -= Ge;
if (bitemp->bpt77) bitemp->bpt77->value += gmf + gpi + Ge;
if (bitemp->bpt88) bitemp->bpt88->value += gmin;
/*
 *  The rhs is entered in
 */
if (bitemp->brhs2)        /* The CN node */
        bitemp->brhs2->rhvalue -= type*iGcrhs;
if (bitemp->brhs3)        /* The CI node */
        bitemp->brhs3->rhvalue += type*( iGcrhs + icrhs);
if (bitemp->brhs5)        /* The BI node */
        bitemp->brhs5->rhvalue += type*ibrhs;
if (bitemp->brhs7)        /* The EI node */
        bitemp->brhs7->rhvalue -= type*( icrhs + ibrhs);


/*
 *  The transient, or charge terms, are added into the
 *  nodal equations.  Note that if only doing a dc analysis
 *  that this sections is skipped.
 */
if (atype == 1) {
        if (bitemp->bpt22) bitemp->bpt22->value += gCsub;
        if (bitemp->bpt28) bitemp->bpt28->value -= gCsub;
        if (bitemp->bpt33) bitemp->bpt33->value += gQbcvbc + gQcvb
        if (bitemp->bpt35) bitemp->bpt35->value -=
                gQbcvbc + gQbcvbe + gQcvbc + gQcvbe;
     if (bitemp->bpt37) bitemp->bpt37->value += gQbcvbe + gQcvbe;
        if (bitemp->bpt53) bitemp->bpt53->value -=
                gQbevbc + gQbcvbc + gQcvbc;
        if (bitemp->bpt55) bitemp->bpt55->value += gQbevbe + gQbeb
                + gQbcvbc + gQbcvbe + gQcvbc + gQcvbe;
        if (bitemp->bpt57) bitemp->bpt57->value -=
                gQbevbe + gQbcvbe + gQcvbe;
        if (bitemp->bpt73) bitemp->bpt73->value += gQbevbc;
   if (bitemp->bpt75) bitemp->bpt75->value -= gQbevbe + gQbevbc;
        if (bitemp->bpt77) bitemp->bpt77->value += gQbevbe;
        if (bitemp->bpt82) bitemp->bpt82->value -= gCsub;
        if (bitemp->bpt88) bitemp->bpt88->value += gCsub;
```

```
                                        /*
                                         *  Now add in the terms for the rhs
                                         */
                                        if (bitemp->brhs2)
                                                bitemp->brhs2->rhvalue -= type*iQsubrhs;
                                        if (bitemp->brhs3)
                                                bitemp->brhs3->rhvalue -= type*(iQbcrhs + iQcrhs);
                                        if (bitemp->brhs5)
                                                bitemp->brhs5->rhvalue += type*(iQberhs
                                                                        +iQbcrhs+iQcrhs)
                                        if (bitemp->brhs7)
                                                bitemp->brhs7->rhvalue -= type*iQberhs;
                                        if (bitemp->brhs8)
                                                bitemp->brhs8->rhvalue -= type*iQsubrhs;
                                }
                                bitemp->ovbiei = vbe;
                                bitemp->ovbici = vbc;
                                bitemp->ogmf = gmf;
                                bitemp->ogmr = gmr;
                                bitemp->ogmu = gmu;
                                bitemp->ogpi = gpi;
                                bitemp->ogQbcvbc = gQbcvbc;
                                bitemp->ogQbcvbe = gQbcvbe;
                                bitemp->ogQbevbe = gQbevbe;
                                bitemp->ogQbevbc = gQbevbc;
                                bitemp->ogQcvbc = gQcvbc;
                                bitemp->ogQcvbe = gQcvbe;

                                bitemp = bitemp->nextbim;
                        }
                }
}

/*
 *  The CapAdmittance routine calculates the term corresponding
 *  to a capacitance ( dQ/dV) to be entered into the admittance
 *  matrix.  This will depend on the type of integration method
 *  used.  Included currently is a backward Euler method (order
 *  = 1) and a trapezoidal method ( order = 2).
 *  The admittance term is the value gcap.
 */
CapAdmittance( gcap, cap)
float *gcap, cap;
{
        extern int order;
        extern float tstep;

        if ( order == 1) {  /* Backward Euler */
                *gcap = cap/tstep;
        }
        else {   /* trapezoidal */
                *gcap = 2.0*cap/tstep;
        }
}

/*
 *  The CapCurrent routine calculates the current corresponding
 *  to the charge ( i=dQ/dt).  This requires knowledge of the
 *  new charge and the old charge (from the previous timestep)
 *  and the old current (if order > 1).
 *  icap is the current calculated.
 *  newq is the new charge.
 *  oldq is the old charge (previous timestep).
 *  oldicap is the old current (previous timestep)
 */
```

CapAdmittance

CapCurrent

```
CapCurrent( icap, newq, oldq, oldicap)
float *icap, newq, oldq, oldicap;
{
        extern int order;
        extern float tstep;

        if (order == 1) { /* Backward Euler */
                *icap = (newq - oldq)/tstep;
        }
        else {  /* Trapezoidal */
                *icap = 2.0*( newq - oldq)/tstep - oldicap;
        }
}
```

curfit

```
curfit( oicc, doicc, icc, iccm)
float *oicc, *doicc, icc, iccm;
{
        float icc2, icc3, iccm2, iccm4, iccm5;

        if (icc <= 0) {
                *oicc = 5.0/( 3.0*iccm);
                *doicc = 0.0;
        }
        else if (icc <= iccm) {
                icc2 = icc*icc;
                icc3 = icc2*icc;
                iccm2 = iccm*iccm;
                iccm4 = iccm2*iccm2;
                iccm5 = iccm4*iccm;
                *oicc = 5.0*(1.0/iccm - icc3/iccm4)/3.0 + icc2*icc2/iccm5;
                *doicc = -5.0*icc2/iccm4 + 4.0*icc3/iccm5;
        }
        else {  /* icc > iccm  */
                *oicc = 1./icc;
                *doicc = -(*oicc)*(*oicc);
        }
}
```

tmjlim

```
/* This is the routine used by Turgeon for limiting
 * the voltage across the junction
 */
tmjlim( vnew, vold, vt, phi)
float *vnew, vold, vt, phi;
{
        float vt10, vt2, vtp2, svnew, deltav;
        float vtemp;

        vt10 = 10.*vt;
        vt2 = 2.*vt;
        vtp2 = .2*vt;
        svnew = *vnew;
        deltav = *vnew - vold;
        if (vold < vt10) *vnew = min( 12.*vt, *vnew);
        if (vold < phi-vt10 && vold >= vt10) {
                vtemp = sign( min( deltav, 5.*vt), deltav);
                *vnew = min( phi - 9.*vt, vold + vtemp);
        }
        if (vold < phi-vt2 && vold >= phi-vt10) {
                vtemp = sign( min( deltav, vt2), deltav);
                *vnew = min( phi - 1.8*vt, vold + vtemp);
        }
        if (vold < phi-vtp2 && vold >= phi-vt2) {
                vtemp = sign( min( deltav, 3.*vtp2), deltav);
                *vnew = min( phi-.18*vt, vold + vtemp);
        }
```

```
        if (vold >= phi-vtp2) {
                vtemp = sign( min( deltav, .05*vt), deltav);
                *vnew = min(.999999*phi, vold + vtemp);
        }
        if (1.-max( abs(*vnew), 1.e-6)/max( abs(svnew),1.e-6) > 0.01)
                ;
                /* printf("limit = 1\n"); */
}
```

REFERENCES

[Ant78] D.A. Antoniadis, S.E. Hansen, and R.W. Dutton, "SUPREM II - A Program for IC Process Modeling and Simulation," Tech. Rep. SEL 78-020, Stanford Electronics Labs, Stanford University, June 1978.

[Eng82] W.L. Engl, R. Laur, and H.K. Dirks, "MEDUSA - A Simulator for Modular Circuits," *IEEE Trans. Computer-Aided Design of ICAS* **CAD-1**, pp. 85-93, April 1982.

[Get76] I.E. Getreu, *Modeling the Bipolar Transistor*, Elsevier Scientific Publishing Company, New York, 1976.

[Gum70a] H.K. Gummel, "A Charge Control Relation for Bipolar Transistors," *Bell Syst. Tech. J.* **49**, pp. 115-120, January 1970.

[Gum70b] H.K. Gummel and H.C. Poon, "An Integral charge Control Model of Bipolar Transistors," *Bell Syst. Tech. J.* **49**, pp. 827-852, May 1970.

[Gyu85] R.S. Gyurcsik, "BIASC: A circuit Simulation Program for the IBM PC," Wescon/85 Professional Program Session Record 32/4, November 1985.

[Hau64] J.R. Hauser, "The Effects of Distributed Base Potential on Emitter-Current Injection Density and Effective Base Resistance for Stripe Transistor Geometries," *IEEE Trans. Electron Devices* **ED-11**, pp. 238-242, May 1964.

[Kir62] C.T. Kirk, "A Theory of Transistor Cutoff Frequency Falloff at High Current Densities," *IRE Trans. Electron Devices* **ED-9**, pp. 164-174, March 1962.

[Kne85] R.W. Knepper, S.P. Gaur, F.Y.Chang, and G.R. Srinivasan, "Advanced Bipolar Transistor Modeling: Process and Device Simulation Tools for Today's Technology," *IBM J. Res. Develop.* 29, pp. 218-228, May 1985.

[Lac82] A.F. Lachner, "Two-Dimensional Integral Analysis of Bipolar Junction Transistors," Ph.D. Dissertation, Department of EECS, University of California, Berkeley, August 1982.

[Mac82] W.D. Mack and M. Horowitz, "Measurement of Series Collector Resistance Bipolar Transistors," *IEEE J. Solid-State Circuits* SC-17, pp. 767-773, August 1982.

[Mey86] R.G. Meyer and R.S. Muller, "Charge-Control Analysis of the Collector-Base Space-Charge-Region Contribution to Bipolar Transistor Transit Time," to be published.

[Mul77] R.S. Muller and T.I. Kamins, *Device Electronics for Integrated Circuits*, Wiley, New York, 1977.

[Nag75] L.W. Nagel, "SPICE2 - A Computer Program to Simulate Semiconductor Circuits", ERL Memo No. ERL-M520, University of California, Berkeley, May 1975.

[Poo69] H.C. Poon, H.K. Gummel, "Modeling of Emitter Capacitance," *Proc. IEEE* 57, pp. 2181-2182, December 1969.

[Rit54] E.S. Rittner, "Extension of the Theory of the Junction Transistor," *Phys. Rev.* 94, pp. 1161-1168, November 1954.

[Sch77] D. Scharfetter, "Bipolar Transistor MODEL for IC Design," in *Process and Device Modeling for Integrated Circuit Design - NATO Advanced Study Institute Series*, Noordhoff Int., The Netherlands, 1977, pp. 365-369.

[Tur80] L.J. Turgeon and J.R. Mathews, "A Bipolar Transistor Model of Quasi-saturation for Use in Computer Aided Design (CAD)," in *IEDM Tech. Dig.*, Washington, DC, December 1980.

[Tur86] L.J. Turgeon and J.R. Mathews, "A Bipolar Transistor Model with Quasi-Saturation for use in Circuit Simulation," to be published.

[War83] R.M. Warner and B.L. Grung, *Transistors, Fundamentals for the Integrated-Circuit Engineer*, Wiley, New York, 1983.

[Web54] W.M. Webster, "On the Variation of Junction-Transistor Current-Amplification Factor with Emitter Current," *Proc. IRE* 42, pp. 914-920, June 1954.

[Whi69] R.J. Whittier and D.A. Tremere, "Current Gain and Cutoff Frequency Falloff at High Currents," *IEEE Trans. Electron Devices* ED-16, pp. 39-57, January 1969.

REFERENCES FROM APPENDIX D

[10] B.R. Chawla and H.K. Gummel, "Transition Region Capacitance of Diffused p-n Junctions," *IEEE Trans. on Electron Devices* ED-18, pp. 178-195, March 1971.

[11] S.M. Sze, *Physics of Semiconductor Devices*, Wiley, New York, 1969, p. 382.

[12] N.H. Fletcher, "General Semiconductor Junction Relations," *J. Electronics*, pp. 609-612, May 1957.

[13] S.R. Dhariwal, L.S. Kotharl, and S.C. Jain, "Saturation of Photovoltage and Photocurrent in p-n Junction Solar Cells," *IEEE Trans. on Electron Devices* ED-23, pp. 504-507, May 1976.